ACR No. L4F16

NATIONAL ADVISORY COMMITTEE FOR AERONAUTICS

WARTIME REPORT

ORIGINALLY ISSUED
June 1944 as
Advance Confidential Report L4F16

EXPERIMENTS ON DRAG OF REVOLVING DISKS, CYLINDERS AND STREAMLINE RODS AT HIGH SPEEDS

By Theodore Theodorsen and Arthur Regier

Langley Memorial Aeronautical Laboratory
Langley Field, Va.

NACA

WASHINGTON

NACA ACR No. L4F16

NATIONAL ADVISORY COMMITTEE FOR AERONAUTICS

ADVANCE CONFIDENTIAL REPORT

EXPERIMENTS ON DRAG OF REVOLVING DISKS, CYLINDERS AND STREAMLINE RODS AT HIGH SPEEDS

By Theodore Theodorsen and Arthur Regier

SUMMARY

An experimental investigation concerned primarily with the extension of test data on the drag of revolving disks, cylinders, and streamline rods to high Mach numbers and Reynolds numbers is presented. A Mach number of 2.7 was reached for revolving rods with Freon 113 as the medium. The tests on disks extended to a Reynolds number of 7,000,000. Parts of the study are devoted to a reexamination of the von Kármán-Prandtl logarithmic resistance law and the Ackeret-Taylor supersonic drag formula and conditions for their validity. The tests confirm, in general, earlier theories and add certain new results. A finding of first importance is that the skin friction does not depend on the Mach number. Of interest, also, are experimental results on revolving rods at very high Mach numbers, which show drag curves of the type familiar from ballistics. A new result which may have general applicability is that the effect of surface roughness involves two distinct parameters, particle size and particle unit density. The particle size uniquely determines the Reynolds number at which the effect of the roughness first appears, whereas the particle unit density determines the behavior of the drag coefficient at higher Reynolds numbers. Beyond the critical Reynolds number at which the roughness effect appears, the drag coefficient is found to be a function of unit density. In the limiting case of particle "saturation," or a maximum density of particles, the drag coefficient remains constant as the Reynolds number is increased.

THEORETICAL BACKGROUND

Von Kármán-Prandtl Theory for Pipes

Measurements of the value of the skin friction between a fluid and a solid constitute one of the means for studying the nature of turbulent flow. Most of the pioneer analytical work in this field is found in the papers by von Kármán (references 1 and 2) and Prandtl (reference 3). The treatment used in the first part of this section follows the work of Prandtl which, in turn, is closely related to the von Kármán papers. The theory, which concerns the flow in pipes, is given in considerable detail as it forms the basis for the succeeding discussion on flat plates, cylinders, and disks. The theoretical work in this section constitutes mainly an attempt to analyze and organize earlier work found in many scattered articles. Considerable work along such lines has already been done by Goldstein, who is responsible for an expression for the drag on revolving disks.

The von Kármán-Prandtl theory for flow in the turbulent layer is based on the following two assumptions:

(1) The ratio of the velocity deficiency to the friction velocity is a function of geometric parameters only.

(2) Adjacent to the wall, but beyond the laminar sublayer, the slope of the curve representing this ratio is inversely proportional to the distance from the wall. The constant of proportionality is a universal constant.

The friction velocity is defined as

$$U_\tau = \sqrt{\frac{\tau_o}{\rho}}$$

and the corresponding friction length is defined as

$$L = \frac{\nu}{U_\tau}$$

(All symbols used in this paper are defined in appendix A.)

A reference time may be given as

$$T = \frac{L}{U_\tau} = \frac{\nu}{U_\tau^2} = \frac{\mu}{\tau_o}$$

The geometric conditions for a pipe are given by one parameter, the radius a. A revolving cylinder of infinite length represents another single-parameter case, in which the reference parameter is the radius of the cylinder.

The equation of motion can be written in the form

$$\frac{u}{U_\tau} = f_1\left(\frac{y}{L}, \frac{t}{T}, \frac{a}{L}\right)$$

and, by adopting suitably defined mean values with respect to time, at a given profile

$$\frac{u}{U_\tau} = f_2\left(\frac{y}{L}, \frac{a}{L}\right)$$

Henceforth u will designate such mean velocity. By measuring the velocity with respect to a velocity U_c in a fixed geometrical position c = ka,

$$\frac{u - U_c}{U_\tau} = f_3\left(\frac{y}{L}, \frac{a}{L}\right)$$

is obtained. About 1930 von Kármán showed that for the turbulent layer this function is essentially independent of L and dependent only on the geometry as indicated in assumption (1); therefore

$$\frac{u - U_c}{U_\tau} = f_3\left(\frac{y}{a}\right)$$

This quite remarkable relationship, which has been generally confirmed by Nikuradse, Wattendorf, and others (references 5 to 7), implies a similarity in the turbulent-field pattern away from the walls at all Reynolds numbers. The basic reason for this similarity remains unknown.

It follows from assumption (2) that near the wall

$$\frac{u - U_\delta}{U_\tau} = f\left(\frac{y}{L}\right)$$

$$= \frac{1}{\kappa} \log \frac{y}{L} + \text{Constant}$$

where $1/\kappa$ is the constant of proportionality. (Natural logarithm has been used throughout except where otherwise indicated.) Since $u = U_\delta$ at $y = \delta$, this relation reduces to

$$\frac{u - U_\delta}{U_\tau} = \frac{1}{\kappa} \log \frac{y}{\delta}$$

This logarithmic relationship holds to a certain value c of the significant parameter a (see fig. 1), where $c = ka$ with k a constant. The value of $1 - k$ is only a small fraction, so that the point c will be relatively close to the wall. The velocity in the center of the pipe is therefore given as the sum of three expressions, that is,

$$\frac{U_{max}}{U_\tau} = \frac{U_\delta}{U_\tau} + \frac{1}{\kappa} \log \frac{c}{\delta} + \left[f\left(\frac{y}{a}\right)\right]_c^a$$

For the laminar sublayer

$$\frac{U_\delta}{U_\tau} = \frac{\delta}{L} = \alpha$$

and the equation may be rewritten as

$$\frac{U_{max}}{U_\tau} = \alpha - \frac{1}{\kappa} \log \alpha + \frac{1}{\kappa} \log \frac{a}{L} + \frac{1}{\kappa} \log \frac{c}{a} + \left[f\left(\frac{y}{a}\right)\right]_c^a$$

$$= C_1 + \frac{1}{\kappa} \log \frac{a}{L} + C_2$$

where

$$C_1 = \alpha - \frac{1}{\kappa} \log \alpha$$

and

$$C_2 = \left[f\left(\frac{y}{a}\right)\right]_c^a + \frac{1}{\kappa} \log \frac{c}{a}$$

The constant C_1 is equal to the nondimensional velocity measured on the logarithmic velocity profile when this curve is extrapolated to $y = L$, and the constant C_2 is the excess velocity in the center of the pipe as compared with that of the logarithmic line extended to $y = c$. (See fig. 1.) When these constants are combined, the following general relation is obtained:

$$\frac{U_{max}}{U_\tau} = C + \frac{1}{\kappa} \log \frac{a}{L}$$

The application of this theory to cases other than circular pipes is restricted to geometric configurations given by a single parameter. It is interesting to observe that both C_1 and $1/\kappa$ are universal constants resulting from the second assumption - namely, that the flow near a wall is a function of the distance from the wall only. The second constant C_2 which gives the excess velocity as compared with the logarithmic distribution at a reference point, the location of which depends on the geometric dimensions involved, is not a universal constant but is dependent on the configuration and the choice of reference length.

The effect of surface roughness may be treated in a similar manner. If the roughness parameter ϵ/L is less than a certain magnitude, there is obviously no effect at all. This value of ϵ/L is found experimentally to be 3.3. For $\frac{\epsilon}{L} > 3.3$, U_{max}/U_τ is shown to be constant, or independent of L, except for the so-called unsaturated condition which will be defined later. Thus

$$\frac{U_{max}}{U_\tau} = C + \frac{1}{\kappa} \log 3.3 \frac{a}{\epsilon}$$

$$= C + \frac{1}{\kappa} \log 3.3 + \frac{1}{\kappa} \log \frac{a}{\epsilon}$$

or

$$\frac{U_{max}}{U_\tau} = K_1 + \frac{1}{\kappa} \log \frac{a}{\epsilon}$$

The velocity distribution is exactly as if there were a laminar layer present of a thickness $\delta \approx 3.9\epsilon$ or as if the length L were $\frac{1}{3.3}\epsilon$. When $L < \frac{1}{3.3}\epsilon$, the velocity distribution no longer changes with an increase in Reynolds number R. It seems, therefore, that the distance from the wall of the innermost disturbance, or the mean value of the thickness of the laminar layer, is of the order of three to four times the height of the irregularities or the grain size ϵ. This fact is not inconsistent with the physical interpretation.

The quantity U_{max}/U_τ is shown to equal $\sqrt{\frac{2}{c_D}}$. Further,

$$L = \frac{\upsilon}{U_\tau}$$

$$= \frac{\upsilon}{U_{max}} \frac{U_{max}}{U_\tau}$$

and, therefore,

$$\frac{a}{L} = R\sqrt{\frac{c_D}{2}}$$

where R is referred to the maximum velocity and is equal to $U_{max}a/\upsilon$. The equation

$$\frac{U_{max}}{U_\tau} = C + \frac{1}{\kappa} \log \frac{a}{L}$$

may thus be written

$$\sqrt{\frac{2}{c_D}} = C + \frac{1}{\kappa} \log R\sqrt{\frac{c_D}{2}}$$

or

$$\frac{1}{\sqrt{c_D}} = C_3 + \frac{1}{\kappa}\frac{1}{\sqrt{2}} \log R\sqrt{c_D}$$

where

$$C_3 = \frac{C - \frac{1}{\kappa}\log\sqrt{2}}{\sqrt{2}}$$

By the similarity hypothesis, the mean velocity in a pipe differs from the maximum value by a constant, or

$$\frac{U_m}{U_\tau} = \frac{U_{max}}{U_\tau} - K_2$$

where U_m is the mean value of the velocity. Prandtl gives 4.07 for the value of K_2. (See reference 3, p. 142.) Note further that the product $R\sqrt{C_D}$ remains the same whether R and C_D refer to the mean or the maximum value of the velocity; therefore,

$$\frac{U_m}{U_\tau} = C - 4.07 + \frac{1}{\kappa}\log R\sqrt{\frac{C_D}{2}}$$

and, finally, with R and C_D referring to the mean velocity,

$$\frac{1}{\sqrt{C_D}} = C_4 + \frac{1}{\kappa}\frac{1}{\sqrt{2}}\log R\sqrt{C_D}$$

where

$$C_4 = \frac{C - 4.07 - \frac{1}{\kappa}\log\sqrt{2}}{\sqrt{2}}$$

With $C = 5.5$ and $\kappa = 0.4$,

$$C_4 \approx 0.4$$

This value is not accurately established, as the various authors seem to differ.

Drag of Flat Plates

In order to obtain the drag formula for flat plates, a calculation similar to the von Kármán-Prandtl treatment

for pipes may be performed. The velocity deficiency Δu is given by the relation

$$\frac{\Delta u}{U_{\tau m}} = f\left(\frac{y}{x}\right)$$

where $U_{\tau m}$ is a mean value between 0 and x, the distance along the plate. The missing momentum may be written as

$$M = \int \rho U^2 \left(1 - \frac{\Delta u}{U}\right) \frac{\Delta u}{U} \, dy$$

or

$$\frac{M}{\rho U^2} = \int_0^{\delta_1} \frac{\Delta u}{U} \, dy - \int_0^{\delta_1} \left(\frac{\Delta u}{U}\right)^2 dy$$

where U is the stream velocity and δ_1 is a significant length giving the thickness of the boundary layer. Rewritten, this equation becomes

$$\frac{M}{\rho U^2} = \frac{U_{\tau m}}{U} \delta_1 \int_0^1 \frac{\Delta u}{U_{\tau m}} \, d\left(\frac{y}{\delta_1}\right) - \left(\frac{U_{\tau m}}{U}\right)^2 \delta_1 \int_0^1 \left(\frac{\Delta u}{U_{\tau m}}\right)^2 d\left(\frac{y}{\delta_1}\right)$$

or, by virtue of the similarity law,

$$\frac{M}{\rho U^2} = \frac{U_{\tau m}}{U} \delta_1 C_5 - \left(\frac{U_{\tau m}}{U}\right)^2 \delta_1 C_6$$

Since the momentum is given directly as

$$M = \frac{1}{2} \rho U^2 C_{Dm} x$$

the following identity is obtained:

$$\frac{1}{2} C_{Dm} x \equiv \sqrt{\frac{C_{Dm}}{2}} \delta_1 C_5 - \frac{C_{Dm}}{2} \delta_1 C_6$$

or

$$\sqrt{\frac{C_{Dm}}{2}} \delta_1 C_5 = \frac{1}{2} C_{Dm} x \left(1 + \frac{\delta_1}{x} C_6\right)$$

which gives

$$\frac{\delta_1}{x} = \frac{1}{C_5} \frac{\sqrt{\frac{C_{Dm}}{2}}}{1 - \frac{C_6}{C_5}\sqrt{\frac{C_{Dm}}{2}}}$$

Using the logarithmic deficiency relation gives for C_5 the value $\frac{1}{\kappa}$, or 2.5, and for C_6/C_5 the value $\frac{2}{\kappa}$, or 5; thus

$$\frac{\delta_1}{x} = \frac{1}{2.5} \frac{\sqrt{\frac{C_{Dm}}{2}}}{1 - 5\sqrt{\frac{C_{Dm}}{2}}}$$

By use of the von Kármán-Prandtl treatment, the stream velocity is obtained in essentially the same form as for pipes. With small adjustments, therefore,

$$\frac{U}{U_{\tau m}} = K_3 + \frac{1}{\kappa} \log \frac{\delta_1 U_{\tau m}}{\upsilon}$$

By use of the expression for δ_1/x, the following equation is obtained:

$$\frac{1}{\sqrt{C_{Dm}}} = K_4 + 4.07 \log_{10} \frac{R_x C_D}{1 - 3.54\sqrt{C_{Dm}}}$$

Local Values of Drag Coefficient for Flat Plates

It may be noted that a relation for the local drag coefficient on a flat plate may be found in a fashion similar to that used later for a disk. Consider a plate of unit width; for the full length l,

$$D = C_D\left(\frac{1}{2}\rho U^2 l\right)$$

$$= \int_0^l C_{Dx}\left(\frac{1}{2}\rho U^2\right)dx$$

With the subscripts m and x referring to mean and local values, respectively, for the length x,

$$\frac{D_x}{\frac{1}{2}\rho U^2} = C_{Dm}x$$

$$= \int_0^x C_{Dx}\,dx$$

or

$$x\frac{dC_{Dm}}{dx} + C_{Dm} = C_{Dx}$$

$$x = \frac{Rv}{U}$$

$$\frac{dC_{Dm}}{\frac{dR}{R}} + C_{Dm} = C_{Dx}$$

$$C_{Dm}\left[\frac{d(\log C_{Dm})}{d(\log R)} + 1\right] = C_{Dx}$$

Therefore

$$C_{Dx} = C_{Dm}(n + 1)$$

where

$$n = \frac{d(\log C_{Dm})}{d(\log R)}$$

Boundary Relation for Revolving Disks

The moment coefficient is defined as

$$C_M = \frac{M}{\frac{1}{2}\rho\omega^2 a^5}$$

The moment may also be written

$$M = 2\rho \int_0^{\delta_1} (2\pi a) u_r u_t a \, dy$$

$$= 2\rho\omega^2 a^5 \left(\frac{U_{\tau m}}{\omega a}\right)^2 \frac{\delta_1}{a} \int_0^1 2\pi \frac{u_r}{U_{\tau m}} \frac{u_t}{U_\tau} d\left(\frac{y}{\delta}\right)$$

$$= \rho\omega^2 a^5 \left(\frac{U_{\tau m}}{\omega a}\right)^2 \frac{\delta_1}{a} C_7$$

where u_r is the variable radial velocity and u_t is the tangential velocity, from which

$$\frac{1}{2} C_M = \left(\frac{U_{\tau m}}{\omega a}\right)^2 \frac{\delta_1}{a} C_7$$

or

$$\frac{\delta_1}{a} \approx \text{Constant}$$

The drag formula then reads

$$\sqrt{\frac{2}{C_D}} = K_5 + \frac{1}{\kappa} \log R\sqrt{C_D}$$

A similar result was obtained by Goldstein in reference 4.

TESTS AND RESULTS

Tests on disks, cylinders, and streamline rods were conducted to determine drag or moment coefficients. For the cylinder the two coefficients are equivalent; for the disk and the rod it is more convenient to employ the moment coefficient, which can be measured directly. In order to extend the range of Mach number, several tests were conducted with Freon 12 or Freon 113 as the medium. The test results obtained are of technical interest because some of the data, particularly for the high Mach number range, were obtained for the first time. It may be pointed out that many of the earlier tests on

revolving disks and, in particular, on revolving cylinders were conducted on a rather small scale and in a limited range of Reynolds number. It may be noted that a considerable range of Reynolds number is generally needed in order to confirm with sufficient reliability a particular theoretical formula. For instance, it may be impossible to obtain a measurable difference between logarithmic or power formulas if a short range of Reynolds number is available. This matter of distinguishing between the various types of formulas is of theoretical interest.

Experiments on Revolving Disks

The moment coefficient is defined as

$$C_M = \frac{M}{\frac{1}{2}\rho\omega^2 a^5}$$

This definition corresponds to the one for laminar flow on a revolving disk given by von Kármán in reference 1 as:

$$C_M = a_1 R^{-\frac{1}{2}}$$

where

$$R = \frac{\omega a^2}{\upsilon}$$

The constant a_1 used by von Kármán was 1.84 for one side or 3.68 for both sides; this value was later adjusted by Cochran (see reference 8, vol. I, p. 112) to $a_1 = 3.87$. If this corrected value of a_1 is inserted, the formula for laminar flow reads

$$C_M = 3.87R^{-\frac{1}{2}}$$

The turbulent-flow formula as given by von Kármán for revolving disks is

$$C_M = 0.146R^{-\frac{1}{5}}$$

In figure 2 are shown the experimental results for tests of a series of revolving disks. The Reynolds

number ranged from about 1600 to more than 1,000,000. Note that the test points lie along the theoretical curves given by the von Kármán formulas. The transition from laminar flow is seen to occur at $R = 310{,}000$. This was the largest value reached with the most highly polished disk.

The thickness of the laminar boundary layer is, according to von Kármán,

$$\delta = 2.58\sqrt{\frac{\nu}{\omega}}$$

or, which is equivalent,

$$\frac{\delta}{a} = 2.58R^{-\frac{1}{2}}$$

Using $R_\delta = \frac{\delta \omega a}{\nu}$ leads to

$$\frac{R_\delta}{R} = \frac{\delta}{a} = 2.58R^{-\frac{1}{2}}$$

For the transition Reynolds number, 310,000,

$$R_\delta = 2.58\sqrt{R}$$
$$= 1440$$

which is of the same order as the minimum critical value obtained for pipes.

Several tests were conducted for the purpose of investigating the factors affecting the transition Reynolds number. The first observation was that the transition Reynolds number could not be increased beyond the value 310,000 no matter how highly the surface was polished or whatever other precautions were taken. Likewise, it was unexpectedly difficult to decrease the transition Reynolds number. The application of coarse sand (60 mesh) glued to the surface of a disk (1-ft radius) only reduced the transition Reynolds number to about 220,000 (fig. 2). The reduction in the transition Reynolds number by initial turbulence was also studied. A small high-pressure air jet applied near the center of the disk produced the greatest observed reduction (fig. 2) and brought the transition to a point near the

intersection of the lines representing the drag formulas for laminar and turbulent flow, which is the absolute minimum. Note that the drag in the turbulent region is quite appreciably increased by surface roughness.

The values of the moment coefficient given in figure 2 represent obviously an integrated drag over the disk. An expression may be obtained for the local drag coefficient C_{Dx} as a function of local Reynolds number as follows:

$$M = C_M\left(\frac{1}{2}\rho\omega^2 a^5\right)$$

$$= 2\int_0^a C_{Dx}\left(\frac{1}{2}\rho\omega^2 r^2\right)\left(2\pi r^2\right) dr$$

$$\frac{M}{\frac{1}{2}\rho\omega^2 a^5} = C_M$$

$$= 4\pi\int_0^1 C_{Dx}\left(\frac{r}{a}\right)^4 d\left(\frac{r}{a}\right)$$

$$C_M\left(\frac{r}{a}\right)^5 = 4\pi\int_0^{r/a} C_{Dx}\left(\frac{r}{a}\right)^4 d\left(\frac{r}{a}\right)$$

$$\frac{dC_M}{d\left(\frac{r}{a}\right)}\left(\frac{r}{a}\right)^5 + 5C_M\left(\frac{r}{a}\right)^4 = 4\pi C_{Dx}\left(\frac{r}{a}\right)^4$$

$$\frac{r}{a}\frac{dC_M}{d\left(\frac{r}{a}\right)} + 5C_M = 4\pi C_{Dx}$$

By substituting

$$r = \sqrt{\frac{R\nu}{\omega}}$$

$$\frac{1}{2\pi} R \frac{dC_M}{dR} + \frac{5}{4\pi} C_M = C_{Dx}$$

or

$$C_{Dx} = \frac{1}{2\pi} C_M \left[\frac{d(\log C_M)}{d(\log R)} + \frac{5}{2} \right]$$

and

$$\log C_{Dx} = \log C_M + \log \frac{K + \frac{5}{2}}{2\pi}$$

where

$$K = \frac{d(\log C_M)}{d(\log R)}$$

If

$$C_M = cR^n$$

then

$$C_{Dx} = \frac{5 + 2n}{4\pi} C_M$$

By use of the expression for log C_{Dx}, some of the data of figure 2 are plotted in figure 3. Although the general picture does not change much, the abrupt nature of the transition becomes apparent.

An illustration of the boundary-layer profiles for various radii or Reynolds numbers is given in figure 4, in which curves of equal velocity $u_t/\omega r$ are also plotted. Note that the thickness of the boundary layer in the laminar region is essentially constant. The transition value of R, 310,000, is shown approximately by the line marked "Approx. transition" in figure 4. The nominal laminar boundary-layer thickness consistently appears to be somewhat in excess of that given by von Kármán in reference 1. There appears to be some discrepancy from the theoretical velocity distribution which is shown for the laminar boundary layer as obtained from work by Cochran. (See reference 8, vol. I, p. 112.) It is recognized that the experimental error in this case is of considerable magnitude. The turbulent boundary layer shows almost perfect agreement with the logarithmic curve, which is plotted for one profile in figure 4.

It may be remarked here that a series of hot-wire tests were run to study fluctuations in the boundary layer with the following results:

(1) No disturbances were noted in the laminar region

(2) A pure tone of a frequency of about 200 cycles per second was observed in the transition region

(3) A random disturbance involving much higher frequencies was observed in the turbulent region

In figure 5 the upper range of the Reynolds number has been considerably extended. The highest Reynolds number reached is 7,000,000. The $\frac{1}{7}$-power law holds fairly well in the observed range which, however, is too limited to permit a distinction between the power law and the logarithmic law for the velocity distribution. The main purpose of the tests, the results of which are shown in figure 5, was to investigate the effect of the Mach number. The first run taken with air as the medium extended to a Reynolds number of about 2,000,000 and a Mach number of 0.62. By using Freon 12 as the medium, the range of Reynolds number was extended to 7,000,000. At the lowest pressure, the highest value of the Mach number reached was 1.69. All the data for Freon 12 show a slightly higher drag than that given by the von Kármán formula, apparently because of some systematic error. The significant result of this investigation is that the drag coefficient is absolutely independent of the Mach number. A separate extension of the experiments to a Mach number of slightly more than two further confirmed this independence of the Mach number.

Experiments on Revolving Cylinders

The experimental results for revolving cylinders are shown in figure 6 as a plot of $\log_{10} C_D$ against $\log_{10} R$, where $R = \frac{\omega a^2}{\nu}$. The drag formula for laminar flow on a revolving cylinder is obtained from Lamb

(reference 9, p. 588) as

$$C_D = \frac{4}{R}$$

where

$$C_D = \frac{D}{qS}$$

$$= \frac{M}{qSa}$$

In this formula S is the surface area and a the radius. In this case it is convenient to use C_D instead of C_M, which was used for the revolving disk, because no integration is involved. The laminar curve is shown in figure 6. The drag relation given by

$$\frac{1}{\sqrt{C_D}} = -0.6 + 4.07 \log_{10} R\sqrt{C_D}$$

for the turbulent flow is also shown in figure 6.

The experimental results are replotted in figure 7, where $\frac{1}{\sqrt{C_D}}$ is shown as a function of $\log_{10} R\sqrt{C_D}$. The relation for the turbulent flow

$$\frac{1}{\sqrt{C_D}} = -0.6 + 4.07 \log_{10} R\sqrt{C_D}$$

appears in figure 7 as a straight line. The coefficient C_D in this formula corresponds to a value of 0.4 for von Kármán's universal constant κ. The relation for the laminar region, $C_D = \frac{4}{R}$ appears as a curved line near the origin.

It is noted that the drag coefficient for rough cylinders is dependent on the relative grain size ϵ/a, where ϵ is the size of the sand and a is the radius of the cylinder (see fig. 8), and that for each grain size the drag coefficient remains constant and

independent of the Reynolds number beyond a certain minimum or critical value, which lies on the line for turbulent flow. In regard to the magnitude of the drag coefficient as a function of relative grain size for particle "saturation" of the surface, it may be remarked that the value of δ is a measure of the thickness of the sublayer or, what amounts to the same thing, a measure of the minimum grain size of the turbulence. It is therefore to be expected that the surface roughness will become effective at the Reynolds number for which ϵ_{cr}, the critical value of ϵ, becomes less than the grain size ϵ. Inversely, it may be seen that, if the Reynolds number becomes smaller than this critical value, the grain size of the turbulence is too large to be affected by the surface roughness. With ϵ greater than ϵ_{cr}, which is 3.3L, the following relation is approximately true for the drag coefficient beyond the critical Reynolds number for surface roughness of saturation density:

$$\frac{1}{\sqrt{C_D}} = -0.6 + 4.07 \log_{10} 3.3\sqrt{2}\,\frac{a}{\epsilon}$$

$$= 2.12 + 4.07 \log_{10} \frac{a}{\epsilon}$$

In figure 9 the experimental points are shown to satisfy this theoretical relation with sufficient accuracy.

Tests were made to determine the effect of the density of spacing of grains of a given size, and the results are presented in figure 10. Such tests were made with a certain unit grain size but with the surface density in grains per square inch varied between 90 and 2200. The grain size used corresponds to the size $\frac{\epsilon}{a} = 0.03$, also used for the preceding experimental results shown in figure 8. It is verified that the critical Reynolds number depends on the grain size only, and it is further shown that the slope of the drag curve beyond the critical Reynolds number is a function of the density. A saturation condition evidently always exists, in which the drag coefficient remains approximately constant and equal to the critical value.

Experiments on Streamline Rods

In figure 11 results are given for certain more or less streamline bodies, each tested in two or more different mediums. The tests were obtained by using actual propellers of 12-inch diameter, which are designated propellers B and C. Propeller B had a section of double symmetry with a circular-arc contour line. Propeller C was obtained by reducing the chord of propeller B by removal of about one-fifth of the chord near one extremity to obtain a blunt-nose airfoil. By running propeller C backwards an airfoil with a blunt trailing edge could also be studied. The drag coefficient used in figures 11, 12, and 13 is the standard torque coefficient used for propellers

$$C_Q = \frac{Q}{\rho n^2 D^5}$$

For the symmetrical airfoil B, a value of the Mach number[1] of about one was reached in air, the range was extended to 1.6 in Freon 12, and the characteristic decrease in the drag coefficient was finally reached in Freon 113. A considerable decrease in drag coefficient was noted at the largest Mach number, 2.7, which to the knowledge of the authors is the highest Mach number reached except for a few cases of projectiles.

The blunt-nose airfoil section C showed approximately the same low-speed resistance as the symmetrical sharp-nose section B but had a maximum torque coefficient very much in excess of that of section B. The test extended only to near the peak of the torque curve with Freon 12 as the medium. By reversing the direction of motion of propeller C to obtain a blunt rear, the expected large increase in drag at low Mach numbers was observed. The appreciable difference in Reynolds number for air and Freon 12 is apparent from the difference in drag coefficients in the range below a Mach number of unity. For higher Mach numbers, the drag coefficient of the section with the blunt rear lies between the drag coefficients of the doubly streamline section and the blunt-nose type; the streamline leading edge is approximately twice as effective as the streamline trailing edge, a result in general agreement with earlier observations. It should be noted, however, that the lowest drag is obtained with both leading and trailing edges streamlined.

[1]Note that the Mach numbers used in figures 11, 12, and 13 are based on the tip radius.

The effect of the Reynolds number is also shown in figure 12, which gives the results of tests to study how the scale effect is superimposed on the Mach number effect. It should be noted again that the Reynolds number effect appears only for a Mach number below unity. A wide variation in the Reynolds number shows no consistent measurable effect on the drag for a Mach number greater than unity. Similar data for a small angle of attack, instead of zero angle of attack as used in the preceding discussion, were used in one case, for which results are given in figure 13.

The four propellers referred to in figures 11 to 13 are shown in a photograph (fig. 14) and the dimensions of the propellers are given in table I.

It is of some interest to interject a superficial analysis of the results presented herein, in view of Ackeret's formula as given by Taylor (reference 10). For the local section Ackeret gives the drag coefficient as

$$C_D = 2\left(\frac{v^2}{a^2} - 1\right)^{-\frac{1}{2}}\left(2\alpha^2 + \overline{\beta_1^2} + \overline{\beta_2^2}\right)$$

where the bar indicates the mean value. For zero angle of attack and a symmetric section with $\overline{\beta_1^2} = \overline{\beta_2^2}$, this relation becomes

$$C_D = 4\left(\frac{v^2}{a^2} - 1\right)^{-\frac{1}{2}}\overline{\beta^2}$$

For a circular-arc section $\overline{\beta^2} = \frac{1}{3}\beta_{max}^2$, where β_{max} is the maximum angle. This angle is, in turn, approximately equal to twice the thickness ratio t, which is the total thickness divided by the chord. For circular-arc sections, therefore,

$$C_D = \frac{16}{3}\left(\frac{v^2}{a^2} - 1\right)^{-\frac{1}{2}}t^2$$

Figure 15 shows C_D plotted against Mach number for different values of t. At M = 1.0, the curves tend erroneously to infinity. This effect follows

from a simplifying assumption used in the derivation of Ackeret's formula.

By using the general form $f(M)$ instead of the Mach number function $\frac{v^2}{a^2} - 1$, the drag coefficient may be written

$$C_D = \frac{16}{3} t^2 f(M)$$

The torque coefficient is known experimentally to be a function of the Mach number, or $1/x_1$, where x_1 is the fraction of radius at which the Mach number is unity; thus, the following integral relation is obtained:

$$C_Q = N\pi^2 \int_0^1 x^3 c\left(\frac{1}{3}t^2\right) f\left(\frac{x}{x_1}\right) dx$$

There are several ways of handling this relation. The nondimensional chord c and the thickness t may be taken to represent a preferred section at approximately 80 percent of the radius. By assuming an initial drag coefficient C_D any desired accuracy may be obtained by iteration methods.

The function $f(M)$ shown in figure 16 has been obtained for propeller B by such a process based on the experimental data given in figure 11. Note that the drag coefficient approaches the value given by the Ackeret formula for large values of M, for which $f(M)$ approaches $(M^2 - 1)^{-\frac{1}{2}}$. Note further that the maximum value of the drag coefficient occurs at $M = 1.2$ with $f(M)$ almost exactly equal to unity. It is, of course, not to be concluded that the function $f(M)$ has general validity; the function is given here for propeller B for the purpose of comparing the data with the Ackeret theory.

CONCLUDING REMARKS

Experimental results on the drag of revolving disks have been presented, which substantiate to a

remarkable degree drag formulas based on the von Kármán-Prandtl theory of skin friction. The range of the investigation was extended to a Mach number of 1.69, which is beyond the range of any earlier test, and to a Reynolds number of 7,000,000. It was established that the skin friction is independent of the Mach number up to this value and appears to be a function of the Reynolds number only.

The drag at supersonic speeds was studied with revolving rods or propeller sections. Mach numbers as high as 2.7 were attained in the tests. The drag at supersonic speeds is a function of the Mach number only, as it appears to be essentially independent of both the Reynolds number and the nature of the medium. The characteristic peak in the drag curve observed for projectiles was obtained. For thin streamline bodies, this peak appears at Mach numbers only slightly beyond unity; in fact, it appears at a Mach number of about 1.2. Systematic tests were conducted on streamline bodies with combinations of sharp and blunt leading and trailing edges for the purpose of obtaining the relative merits of such features. It was found that the increase in the peak value of the drag coefficient resulting from a blunt nose is about twice that resulting from a blunt trailing edge, when both drag coefficients are compared with the drag coefficient of a section with streamline leading and trailing edges, which has the lowest value.

Significant results were obtained on revolving free cylinders for which references to earlier tests seem to be lacking. It was found that, at very low Reynolds numbers, the drag asymptotically approaches the laminar drag of the classical theory whereas, at higher Reynolds numbers, the drag is found to conform to a logarithmic formula of the von Kármán type. There is no distinct transition from laminar to turbulent flow, as is found in pipes and on revolving disks. The flow is essentially turbulent down to the smallest Reynolds numbers.

The effect of initial turbulence was particularly studied in connection with tests of revolving disks. It was found that the transition Reynolds number was very slightly affected. The critical Reynolds number at which the roughness effect appears depends on particle size only and is not a function of particle

density. Beyond this value of the Reynolds number, the drag coefficient is constant only when the surface is "saturated," that is, when the density of the individual particles attains a maximum value. For a roughness of less than this particle density, the drag coefficient decreases with Reynolds number.

It is interesting further to note the persistence of the logarithmic relationship. When $1/\sqrt{C_D}$ is plotted as a function of $\log R\sqrt{C_D}$ (where C_D is the drag coefficient and R is the Reynolds number), the lines representing turbulent flow are invariably straight. A rather critical demonstration of the logarithmic velocity pattern near the surface is thus shown. The range investigated is of considerable extent.

Langley Memorial Aeronautical Laboratory
National Advisory Committee for Aeronautics
Langley Field, Va.

APPENDIX A

SYMBOLS

U_τ	friction velocity $\left(\sqrt{\frac{\tau_o}{\rho}}\right)$
τ_o	shear per unit area at surface
ρ	mass of air per unit volume
$U_{\tau m}$	mean friction velocity (from 0 to x)
U	stream velocity for flat plates
U_{max}	maximum velocity
U_m	mean velocity (in pipes)
U_c	reference velocity (at a given fraction of radius or of other reference dimension)
U_δ	velocity at δ
u	absolute variable velocity of fluid in boundary layer
Δu	velocity deficiency, stream velocity minus local velocity for flat plates
u_r	radial velocity for disks
u_t	tangential velocity for disks
ω	angular velocity, radians
δ	thickness of laminar sublayer
δ_1	boundary-layer thickness
L	friction length (ν/U_τ)
l	total length of plate
T	reference time (L/U_τ)
t	time; also, thickness ratio for propeller section, $\frac{\text{thickness of airfoil}}{\text{chord}}$

ν coefficient of kinematic viscosity

μ coefficient of viscosity

r variable radius of pipe, disk, or propeller

a radius of pipe, cylinder, or disk; also, velocity of sound in fluid

x distance from leading edge of flat plate in direction of flow: also, fraction of propeller radius ($x = \frac{r}{R}$ where R denotes radius of propeller tip)

x_1 fraction of propeller radius at which Mach number is unity

y distance normal to surface

$\kappa, \frac{1}{\kappa}$ nondimensional profile constant for turbulent flow near walls

c fraction of reference dimension $\left(\frac{c}{a} = k\right)$; also, nondimensional chord of airfoil, $\frac{\text{chord}}{\text{radius}}$

α angle of attack of airfoil; also, profile constant (δ/L)

C_D total-drag coefficient (Many authors use f, φ, or $\frac{\lambda}{4}$ instead of C_D for pipes)

C_{Dm} mean drag coefficient (from 0 to x)

C_{Dx} local drag coefficient

D drag; also, propeller diameter

D_x drag of plate (from 0 to x)

ϵ grain size of roughness

ϵ_{cr} grain size of critical roughness for particular value of drag coefficient

C_M moment coefficient for revolving disks

M missing momentum; moment for disks; or Mach number

R	Reynolds number
R_δ	Reynolds number based on thickness of boundary layer
R_x	Reynolds number based on distance from leading edge of flat plate or on local radius of disk
R_d	Reynolds number based on pipe diameter
R_a	Reynolds number based on pipe radius
v	velocity (Ackeret formula)
q	dynamic pressure (for cylinders, $q = \frac{1}{2}\rho\omega^2a^2$)
S	area of cylinder
C_Q	torque coefficient $(Q/\rho n^2D^5)$
Q	torque
N	number of blades
n	rotational speed, revolutions per second; also, coefficient in power law
β_1,β_2	angles which upper and lower surfaces of airfoil make with center line
β_{max}	maximum angle which circular-arc section makes with center line
C_1	nondimensional velocity measured on logarithmic velocity profile when this curve is extrapolated to $y = L$
C_2	nondimensional excess velocity at $y = a$ over that of logarithmic line extended to $y = a$
$C = C_1 + C_2$	
$C_3,C_4,\ldots$	constants
$K_1,K_2,K_3,\ldots$	constants
k	constant
a_1	constant in equation for moment coefficient of revolving disks

APPENDIX B

NUMERICAL VALUES OF POWER REQUIREMENTS FOR REVOLVING DISKS AND CYLINDERS

A chart is presented (fig. 17) which gives the horsepower required to drive a smooth disk in standard air (760 mm and 15° C, $\rho = 0.00238$ slugs/cu ft and $\nu = 0.000159$ ft^2/sec). Lines of constant horsepower ranging in value from 0.01 to 1000 are plotted with disk rotational speed (in rpm) as abscissa and disk diameter (in ft) as ordinate. The dashed line in figure 17 represents a Reynolds number of about 400,000, which is considered the transition Reynolds number.

The following formulas were used to calculate the power for disks operating in the turbulent region:

$$M\omega = C_M\left(\frac{1}{2}\rho a^5\omega^3\right)$$

$$C_M = 0.146R^{-\frac{1}{5}}$$

$$= 0.146\,\frac{\omega^{-\frac{1}{5}}a^{-\frac{2}{5}}\rho^{-\frac{1}{5}}}{\mu^{-\frac{1}{5}}}$$

$$\text{Horsepower} = \frac{M\omega}{550}$$

$$= \frac{0.146}{550 \times 2}\rho^{0.8}a^{4.6}\omega^{2.8}\mu^{0.2}$$

Inasmuch as the formula for C_M is based on the $\frac{1}{7}$ power for velocity distribution, the calculated values of C_M are too low for high Reynolds numbers. This error may become appreciable for the highest power, since the chart (fig. 17) covers a range of Reynolds numbers to 60,000,000.

A chart is also presented (fig. 18) which gives the horsepower required to rotate a smooth cylinder of unit length (1 ft) in standard air. The following formulas have been used in calculating the curves:

$$M\omega = C_{Dq}Sa\omega$$

$$= 2\pi a \frac{C_D \rho \omega^2 a^2}{2} l a \omega$$

$$\text{Horsepower} = \frac{M\omega}{550}$$

$$= \frac{C_D \pi \rho a^4 \omega^3}{550}$$

where, for smooth cylinders,

$$\frac{1}{\sqrt{C_D}} = -0.6 + 4.07 \log_{10} R\sqrt{C_D}$$

and, for rough cylinders, $\epsilon > \epsilon_{cr}$,

$$\frac{1}{\sqrt{C_D}} = 2.12 + 4.07 \log_{10} \frac{a}{\epsilon}$$

APPENDIX C

COLLECTED SKIN-FRICTION FORMULAS

FLAT PLATES (ONE SIDE)

Symbols

The following symbols are used in the formulas for flat plates collected herein:

C_D total drag coefficient

C_{Dx} local drag coefficient at point x

x distance from leading edge of flat plate in direction of flow

l length of flat plate in direction of flow

R Reynolds number based on l

R_x Reynolds number based on x

Laminar Flow

The formula for total drag coefficient

$$C_D = 1.328R^{-\frac{1}{2}}$$

is based on the simplified hydrodynamic equations developed by Prandtl in 1904. (See reference 2, p. 2.) The constant, which was calculated by Blasius in 1908 as 1.327, was calculated by Töpfer in 1912 as 1.328. (See reference 3, p. 89.) The formula for local drag coefficient is

$$C_{Dx} = 0.664R_x^{-\frac{1}{2}}$$

Von Kármán, Schoenherr, and others have indicated that, if the total drag coefficient is

$$C_D = \text{Constant } R^n$$

the local drag coefficient is given as

$$C_{Dx} = (n + 1)C_D$$

This relation is derived in the section entitled "Local Values of Drag Coefficient for Flat Plates" in this paper. All formulas given in this appendix for the local drag on flat plates are in conformity with this derivation.

Turbulent Flow - Smooth Surface

The formulas

$$C_D = 0.074R^{-\frac{1}{5}}$$

and

$$C_{Dx} = 0.059R_x^{-\frac{1}{5}}$$

were first calculated by von Kármán in 1920. (See references 1 and 2.) Based on results from pipes and on the $\frac{1}{7}$-power law for velocity distribution, they are consequently valid in the lower Reynolds number range, $R < 10,000,000$.

Some writers use the following formulas of the same type, which are fairly accurate to a Reynolds number of 500,000,000:

$$C_D = 0.072R^{-\frac{1}{7}}$$

$$C_{Dx} = 0.026R_x^{-\frac{1}{7}}$$

Of more general validity are the so-called logarithmic drag formulas of the type

$$\frac{1}{\sqrt{C_D}} = 4.15 \log_{10} RC_D$$

The form of this relation was determined by von Kármán with constants adjusted to conform with data by Schoenherr and others. (See reference 2, p. 12.) In the present paper a different form has been developed, which is in somewhat stricter theoretical conformity with the physical relations involved:

$$\frac{1}{\sqrt{C_D}} = 4.07 \log_{10} \frac{RC_D}{1 - 3.54\sqrt{C_D}}$$

Prandtl has developed an explicit expression which gives essentially the same results as the logarithmic formulas. It is

$$C_D = 0.455(\log_{10} R)^{-2.58}$$

(See reference 3, p. 153.) The local drag coefficient has also been given by von Kármán in a logarithmic form with the constants adjusted to fit the experiments of Kemp, which included measurements on small movable plates inserted on a long pontoon. This formula is

$$\frac{1}{\sqrt{C_{Dx}}} = 1.7 + 4.15 \log_{10} R_x C_{Dx}$$

(See reference 2, p. 12.)

Turbulent Flow - Rough Surface

Schlichting (see reference 8, p. 382) gives the two following formulas for the total and the local drag coefficients for rough flat plates, respectively:

$$C_D = \left(1.89 + 1.62 \log_{10} \frac{x}{\epsilon}\right)^{-2.5}$$

$$C_{Dx} = \left(2.87 + 1.58 \log_{10} \frac{x}{\epsilon}\right)^{-2.5}$$

Von Kármán (reference 2, p. 18) gives for the local drag coefficient for rough surfaces a formula of the logarithmic type

$$\frac{1}{\sqrt{C_{Dx}}} = 5.8 + 4.15 \log_{10} \frac{x}{\epsilon}\sqrt{C_{Dx}}$$

PIPES

Symbols

The symbol R_d used in this section refers to the Reynolds number based on the pipe diameter and the mean flow velocity, and the symbol R_a refers to the Reynolds number based on pipe radius. Some writers use f or γ instead of C_D, used herein, and others use λ where $\lambda = 4C_D$.

Laminar Flow

For laminar flow in pipes the formula for drag coefficient is

$$C_D = \frac{16}{R_d}$$

This formula is attributed to Poiseuille and Wiedeman. (See reference 3, p. 38, and reference 8, p. 298.)

Turbulent Flow - Smooth Surface

The formula for drag coefficient for turbulent flow in smooth pipes is

$$C_D = 0.079 R_d^{-\frac{1}{4}}$$

This formula is based on the experimental work of Blasius (see reference 3, p. 136), for which the Reynolds number range was rather limited. Later work by Nikuradse (reference 5) extended the range of Reynolds number to a much higher value. The following formula of the type developed by von Kármán fits the data better:

$$\frac{1}{\sqrt{C_D}} = -0.40 + 4.00 \log_{10} R_d \sqrt{C_D}$$

(See reference 8, p. 338.) In the present paper a formula of this type with different constants is developed:

$$\frac{1}{\sqrt{C_D}} = 0.40 + 4.07 \log_{10} R_d \sqrt{C_D}$$

Turbulent Flow - Rough Surface

For turbulent flow in rough pipes

$$\frac{1}{\sqrt{C_D}} = 3.46 + 4.00 \log_{10} \frac{a}{\epsilon}$$

The experimental work in deriving this formula was done by Nikuradse. (See reference 8, p. 380 and reference 6.)

REVOLVING DISKS

Symbols

The following symbols are used in the formulas for revolving disks:

C_M moment coefficient

C_{Dx} local drag coefficient at radius x

R_x Reynolds number at radius x $\left(\frac{\omega x^2}{\nu}\right)$

Laminar Flow

For laminar flow

$$C_M = 3.87R^{-\frac{1}{2}}$$

and

$$C_{Dx} = \frac{3.87}{\pi} R_x^{-\frac{1}{2}}$$

This formula for local drag coefficient is derived from the relation

$$C_{Dx} = \frac{5 + 2n}{4\pi} C_M$$

For the development of this relation and for references, see the section entitled "Experiments on Revolving Disks" in this paper.

Turbulent Flow

For turbulent flow

$$C_M = 0.146R^{-\frac{1}{5}}$$

and

$$C_{Dx} = 0.053R_x^{-\frac{1}{5}}$$

The formula for the local drag coefficient C_{Dx} is derived from the equation for the moment coefficient C_M in the same way as for the case of laminar flow. The local drag coefficient in logarithmic form may be given as

$$\frac{1}{\sqrt{C_{Dx}}} = -2.05 + 4.07 \log_{10} R_x \sqrt{C_D}$$

The constant -2.05 has been adjusted to fit the data of figure 3.

REVOLVING CYLINDERS

For laminar flow

$$C_D = \frac{4}{R}$$

For turbulent flow on smooth cylinders

$$\frac{1}{\sqrt{C_D}} = -0.6 + 4.07 \log_{10} R \sqrt{C_D}$$

For turbulent flow on rough cylinders

$$\frac{1}{\sqrt{C_D}} = 2.1 + 4.0 \log_{10} \frac{a}{\epsilon}$$

The development of these formulas and the references are given in the section entitled "Experiments on Revolving Cylinders."

REFERENCES

1. von Kármán, Th.: Über laminare und turbulente Reibung. Z.f.a.M.M., Bd. 1, Heft 4, Aug. 1921, pp. 233-252.

2. von Kármán, Th.: Turbulence and Skin Friction. Jour. Aero. Sci., vol. 1, no. 1, Jan. 1934, pp. 1-20.

3. Prandtl, L.: The Mechanics of Viscous Fluids. Vol. III of Aerodynamic Theory, div. G, W. F. Durand, ed., Julius Springer (Berlin), 1935, pp. 34-208.

4. Goldstein, S.: On the Resistance to the Rotation of a Disc Immersed in a Fluid. Proc. Cambridge Phil. Soc., vol. XXXI, pt. II, April 1935, pp. 232-241.

5. Nikuradse, J.: Gesetzmässigkeiten der turbulenten Strömung in glatten Rohren. Forschungsheft 356, Forschung auf dem Gebiete des Ingenieurwesens, Ausg. B, Bd. 3, Sept.-Oct. 1932.

6. Nikuradse, J.: Strömungsgesetze in rauhen Rohren. Forschungsheft 361, Beilage zu Forschung auf dem Gebiete des Ingenieurwesens, Ausg. B, Bd. 4, July-Aug. 1933.

7. Wattendorf, F. L.: A Study of the Effect of Curvature on Fully Developed Turbulent Flow. Proc. Roy. Soc. (London), ser. A, vol. 148, no. 865, Feb. 1935, pp. 565-598.

8. Fluid Motion Panel of the Aeronautical Research Committee and Others: Modern Developments in Fluid Dynamics. Vols. I and II. S. Goldstein, ed., Oxford at the Clarendon Press, 1938.

9. Lamb, Horace: Hydrodynamics. Sixth ed., Cambridge Univ. Press, 1932.

10. Taylor, G. I.: Applications to Aeronautics of Ackeret's Theory of Aerofoils Moving at Speeds Greater Than That of Sound. R. & M. No. 1467. British A.R.C., 1932.

TABLE I

DIMENSIONS OF PROPELLERS OR REVOLVING RODS

FOR TESTS AT HIGH MACH NUMBERS

[All propellers have a straight taper in chord and thickness. The tips are rounded as shown in fig. 14.]

Propeller designation	Airfoil section	Pitch (deg)	At 50 percent radius		At 92 percent radius	
			Chord (in.)	Thickness (in.)	Chord (in.)	Thickness (in.)
B	Circular arc	0	1.75	0.31	1.07	0.14
C	Blunt nose	0	1.30	.35	.82	.15
D	Circular arc	[a]2.5	1.44	.18	1.03	.11
E	Circular arc	0	.83	.13	.52	.07

[a]Propeller D was twisted so that approximately the outer half of the blade had an angle of attack.

NATIONAL ADVISORY
COMMITTEE FOR AERONAUTICS

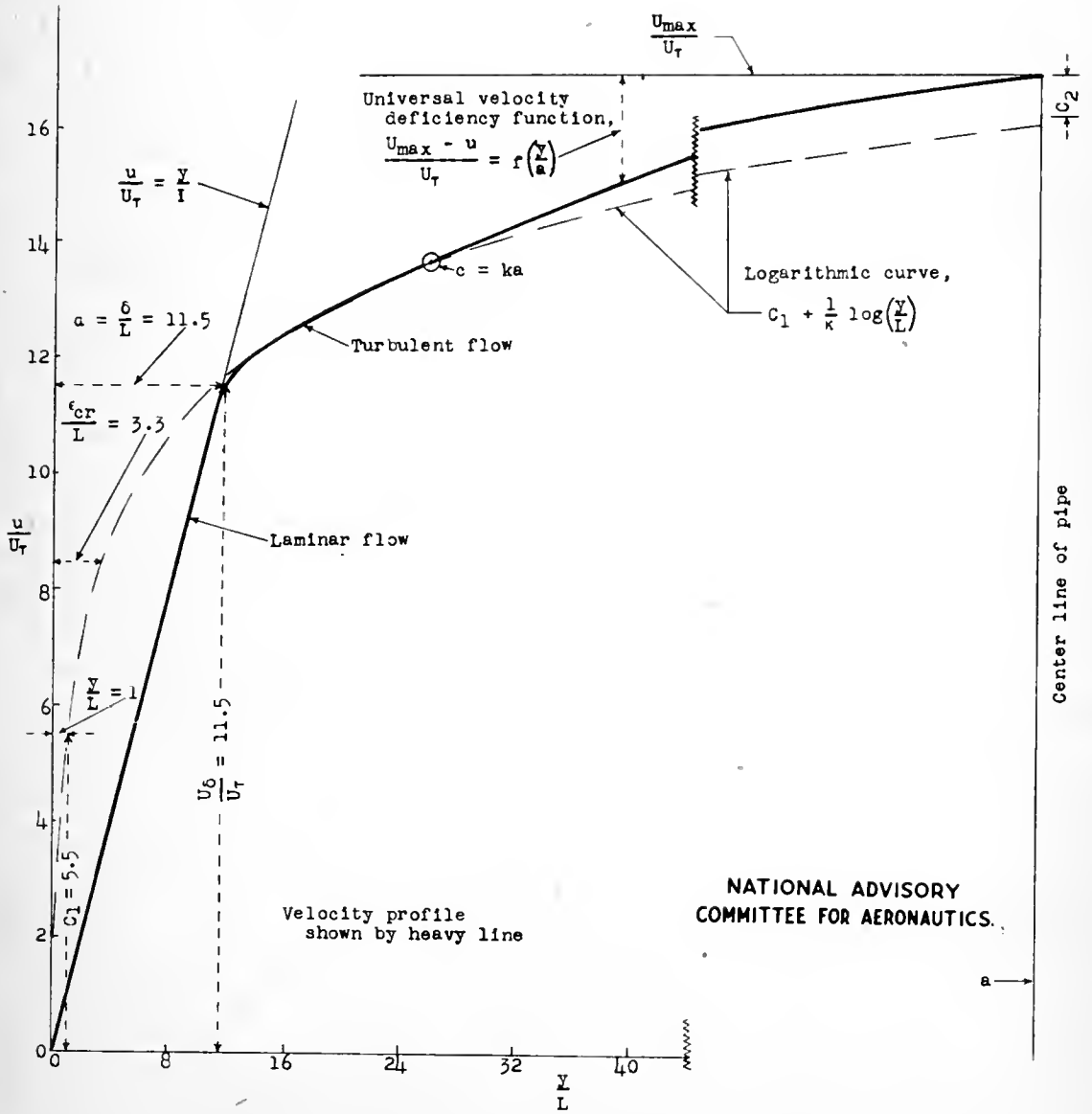

Figure 1.- Parameters and functions of the velocity profile by the von Kármán-Prandtl theory.

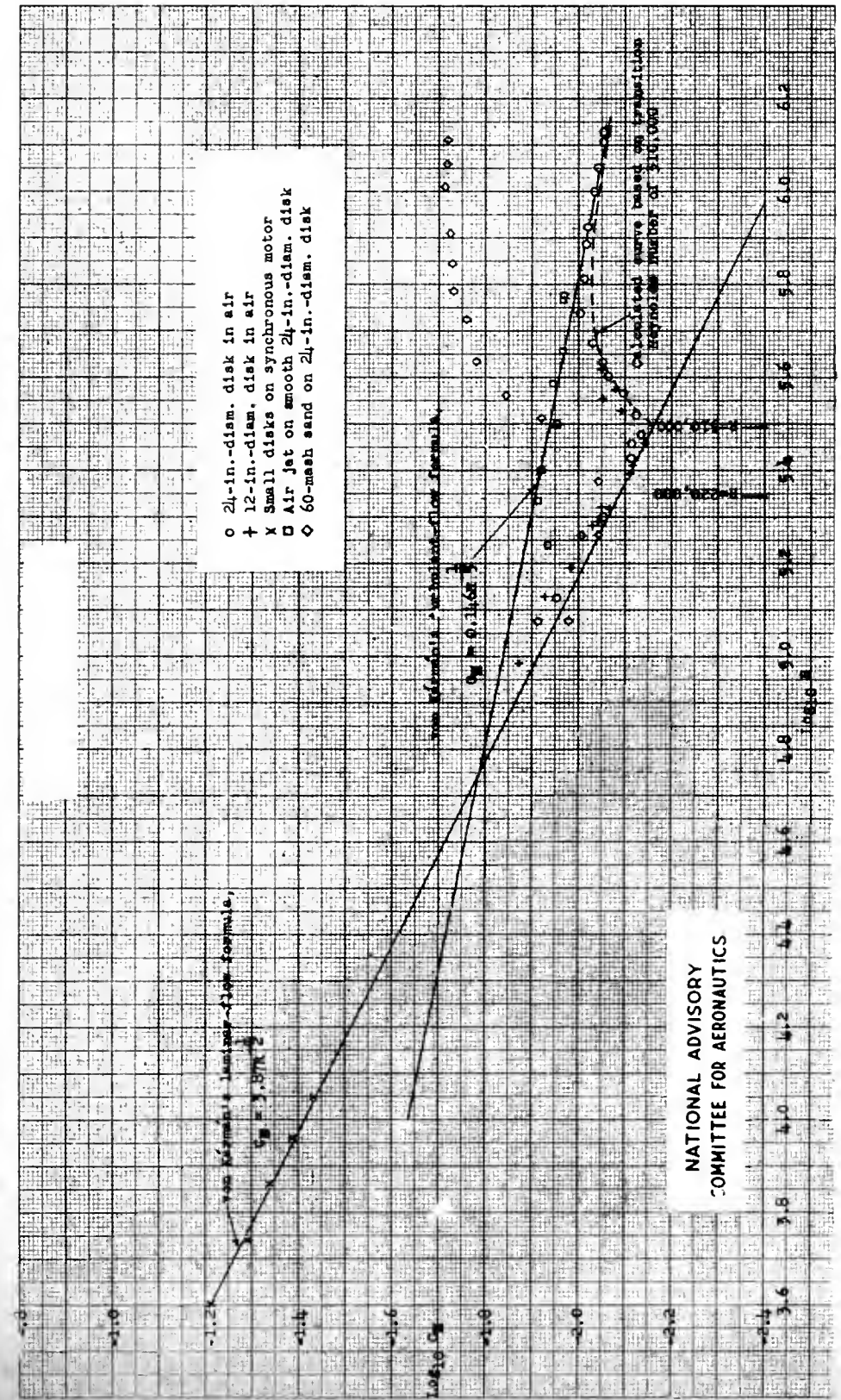

Figure 2.- Moment coefficient $C_M = \frac{M}{\frac{1}{2}\rho\omega^2 a^5}$ for disks as function of Reynolds number.

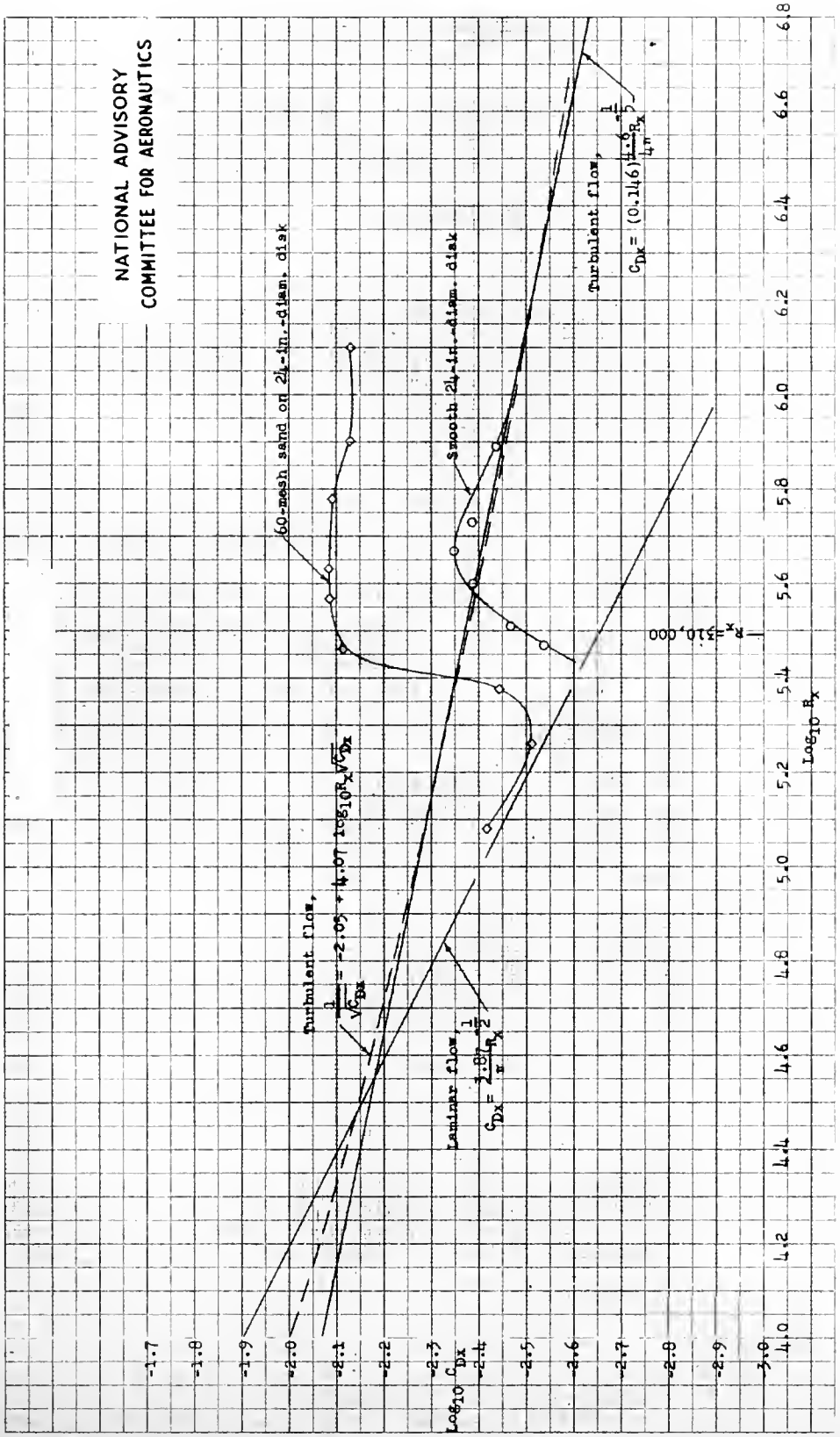

Figure 3.- Local drag coefficient for disks obtained by differentiating the moment-coefficient curve.

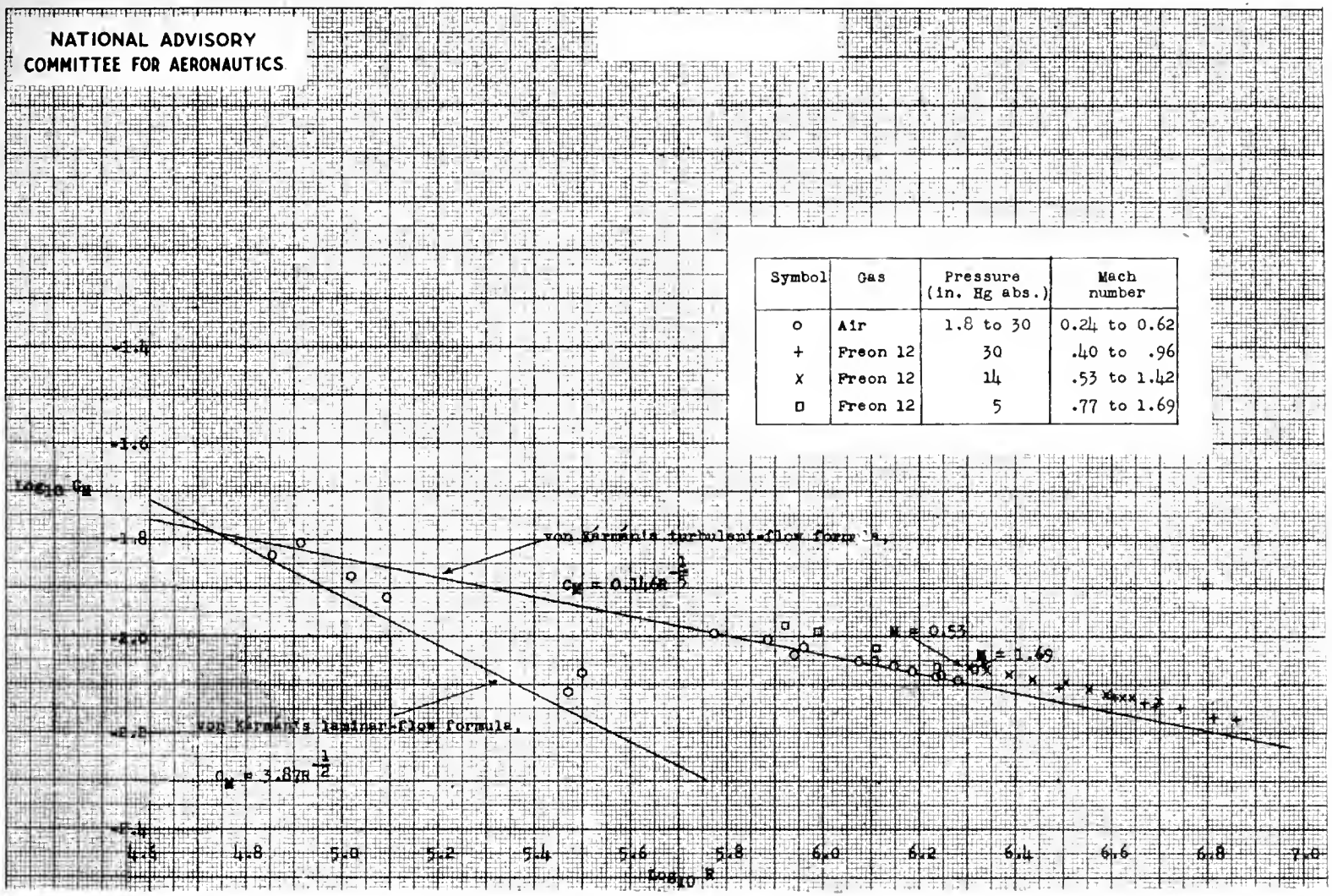

Figure 5.- Moment coefficient for disks as function of Reynolds number for several values of Mach number with air and Freon 12 as mediums. Maximum Mach number, 1.69.

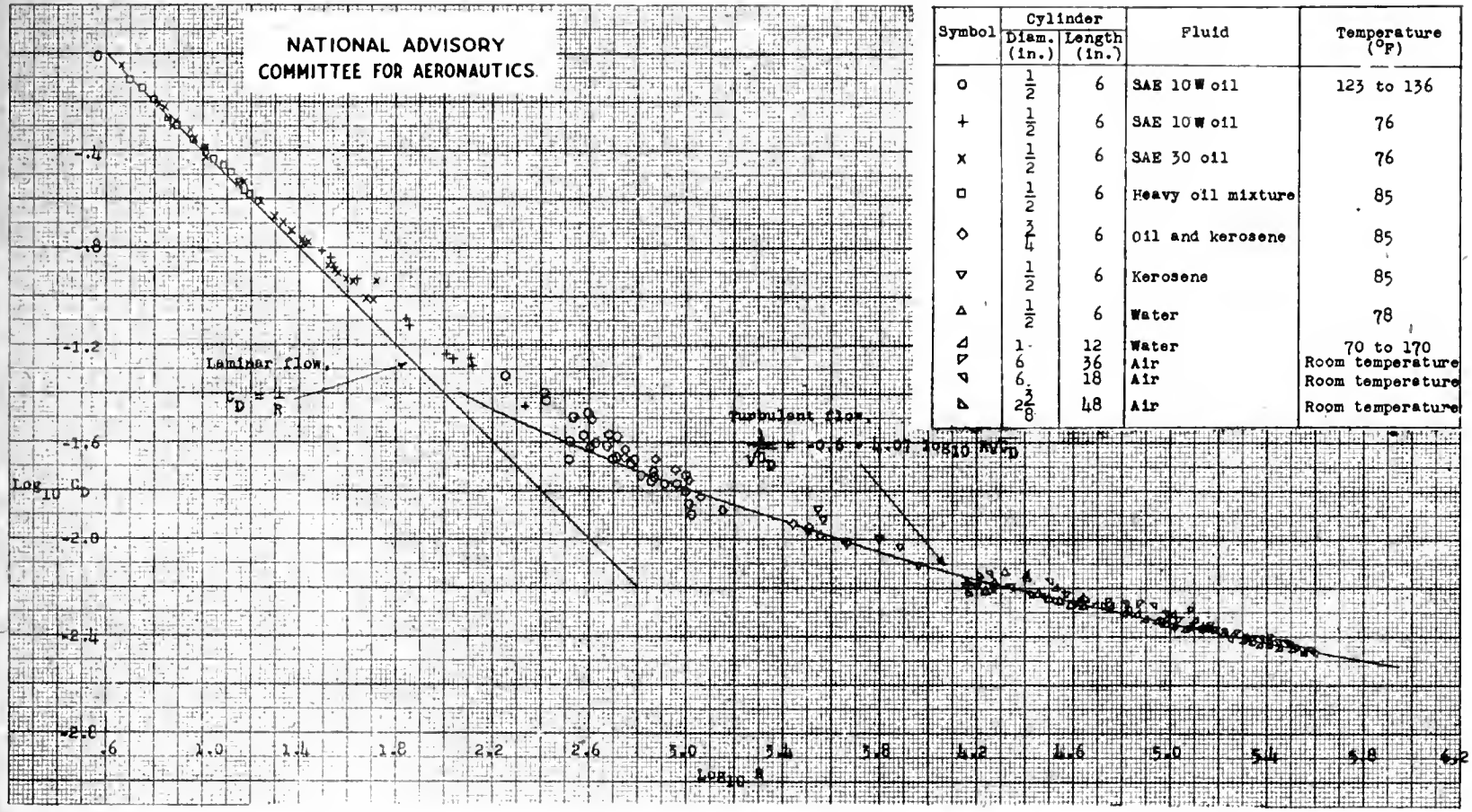

Symbol	Cylinder Diam. (in.)	Cylinder Length (in.)	Fluid	Temperature (°F)
○	$\frac{1}{2}$	6	SAE 10W oil	123 to 136
+	$\frac{1}{2}$	6	SAE 10W oil	76
×	$\frac{1}{2}$	6	SAE 30 oil	76
□	$\frac{1}{2}$	6	Heavy oil mixture	85
◇	$\frac{3}{4}$	6	Oil and kerosene	85
▽	$\frac{1}{2}$	6	Kerosene	85
△	$\frac{1}{2}$	6	Water	78
◁	1	12	Water	70 to 170
▷	6	36	Air	Room temperature
▽	6	18	Air	Room temperature
△	$2\frac{3}{8}$	48	Air	Room temperature

Figure 6.- Drag coefficient $C_D = \frac{M}{qSa}$ for cylinders as function of Reynolds number.

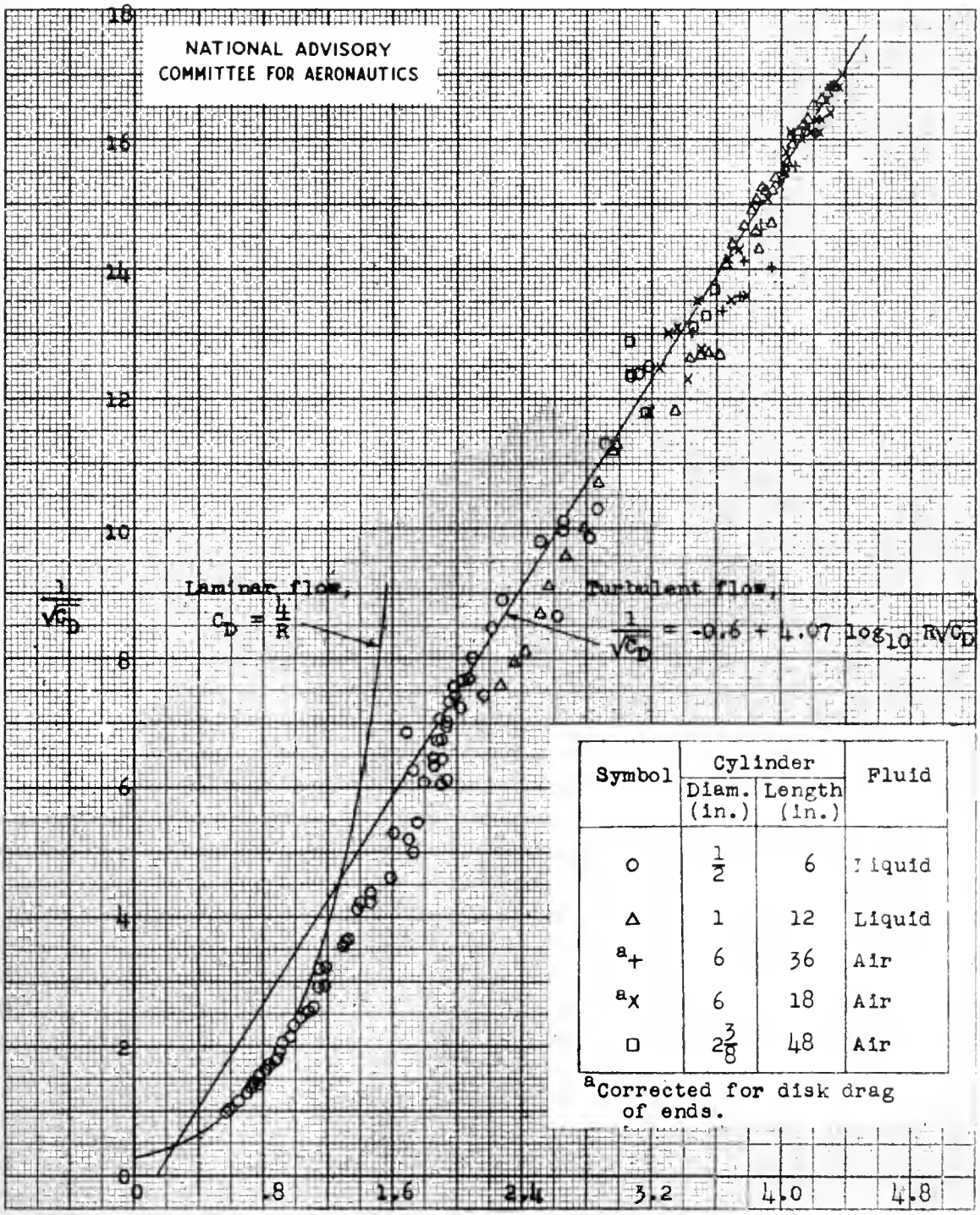

Symbol	Cylinder		Fluid
	Diam. (in.)	Length (in.)	
○	$\frac{1}{2}$	6	Liquid
△	1	12	Liquid
[a]+	6	36	Air
[a]×	6	18	Air
□	$2\frac{3}{8}$	48	Air

[a]Corrected for disk drag of ends.

Figure 7.- Drag parameter $\frac{1}{\sqrt{C_D}}$ for smooth cylinders as function of $\log_{10} R\sqrt{C_D}$.

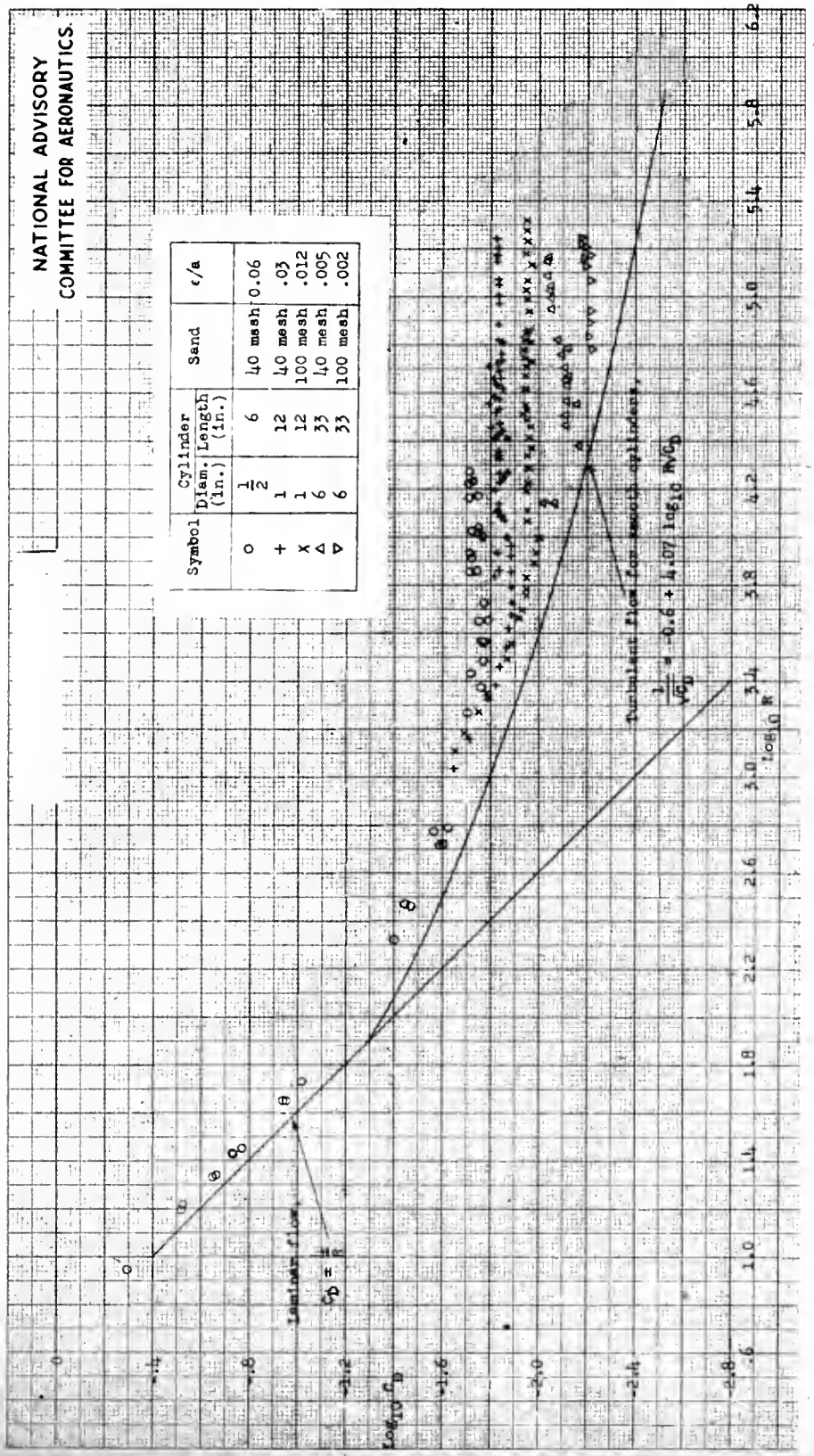

Figure 8.- Effect of surface roughness, or grain size, on the drag coefficient.
Saturation density of particles.

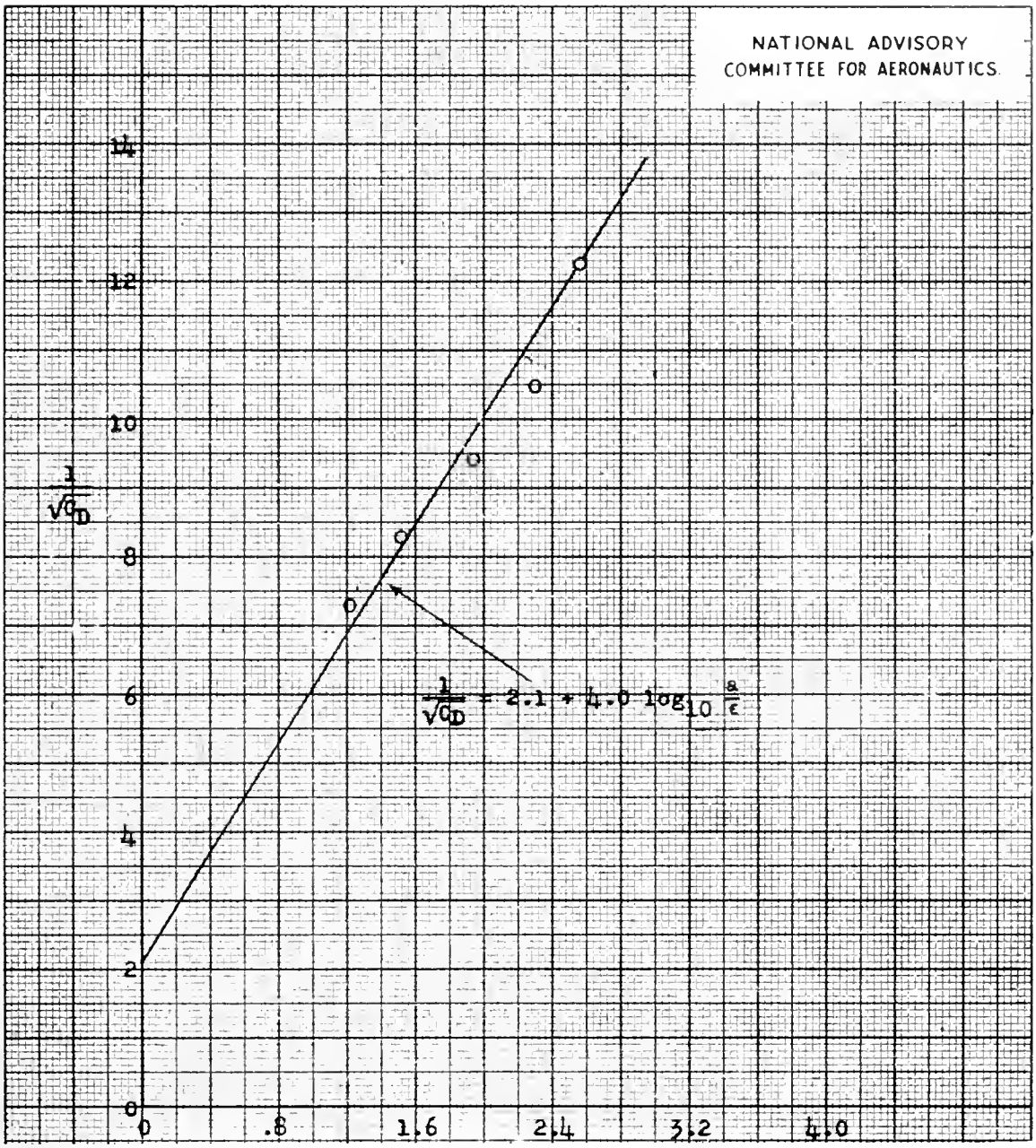

Figure 9.- Drag parameter $\frac{1}{\sqrt{C_D}}$ for rough-surfaced cylinders as function of $\log_{10} \frac{a}{\epsilon}$.

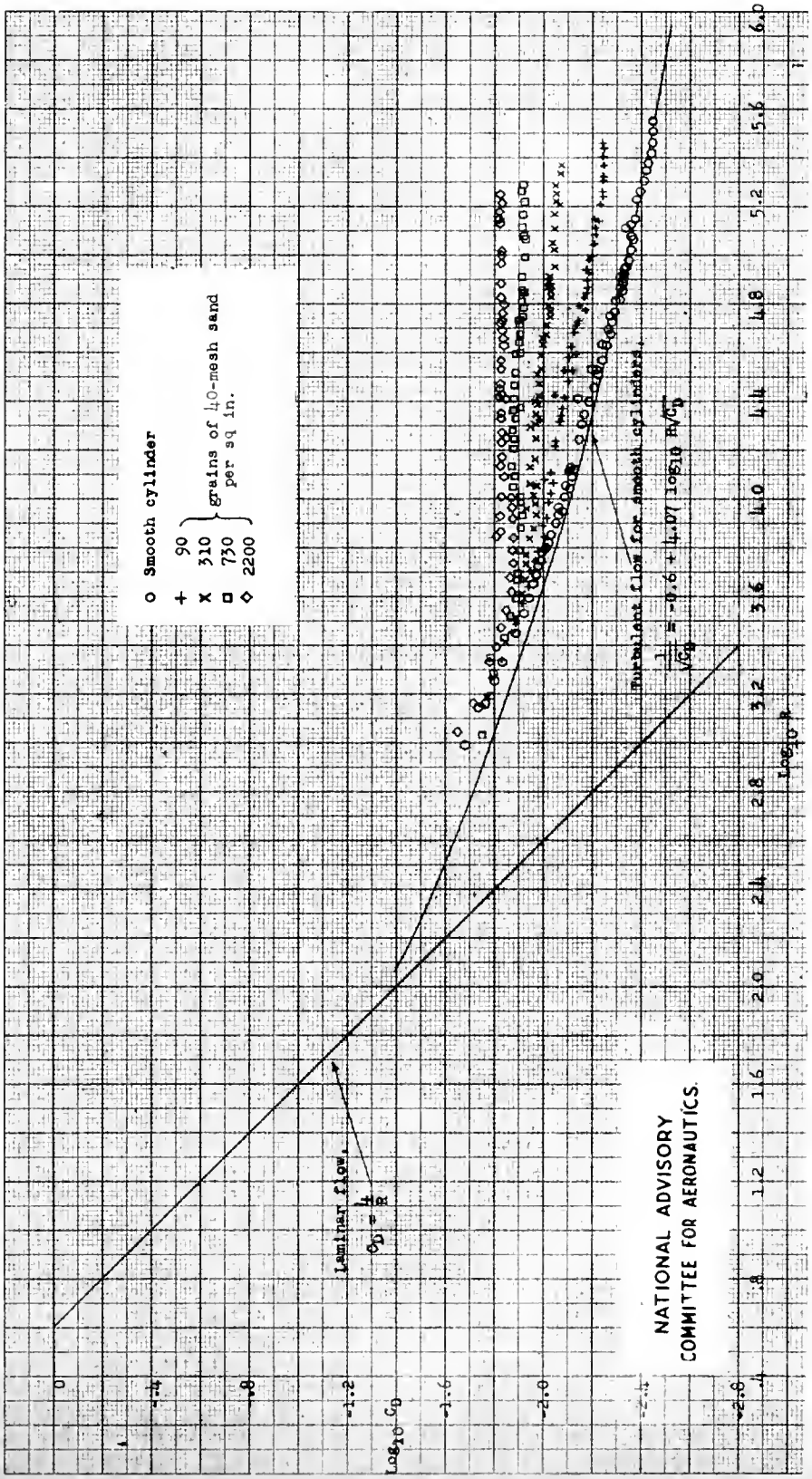

Figure 10.- Effect of varying density of surface roughness on the drag coefficient.

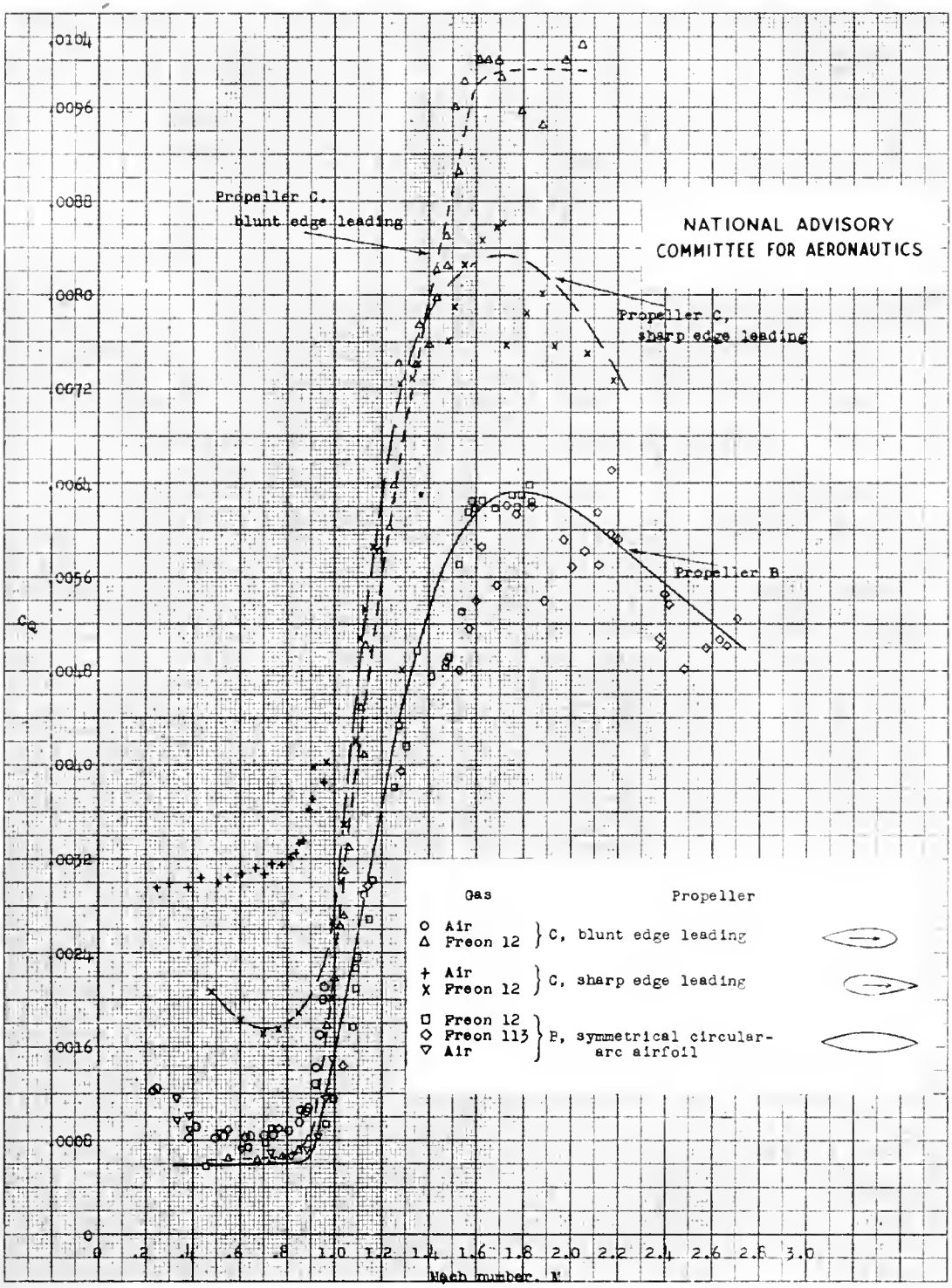

Figure 11.- Torque coefficient $C_Q = \frac{Q}{\rho n^2 D^5}$ as function of Mach number for propellers B and C.

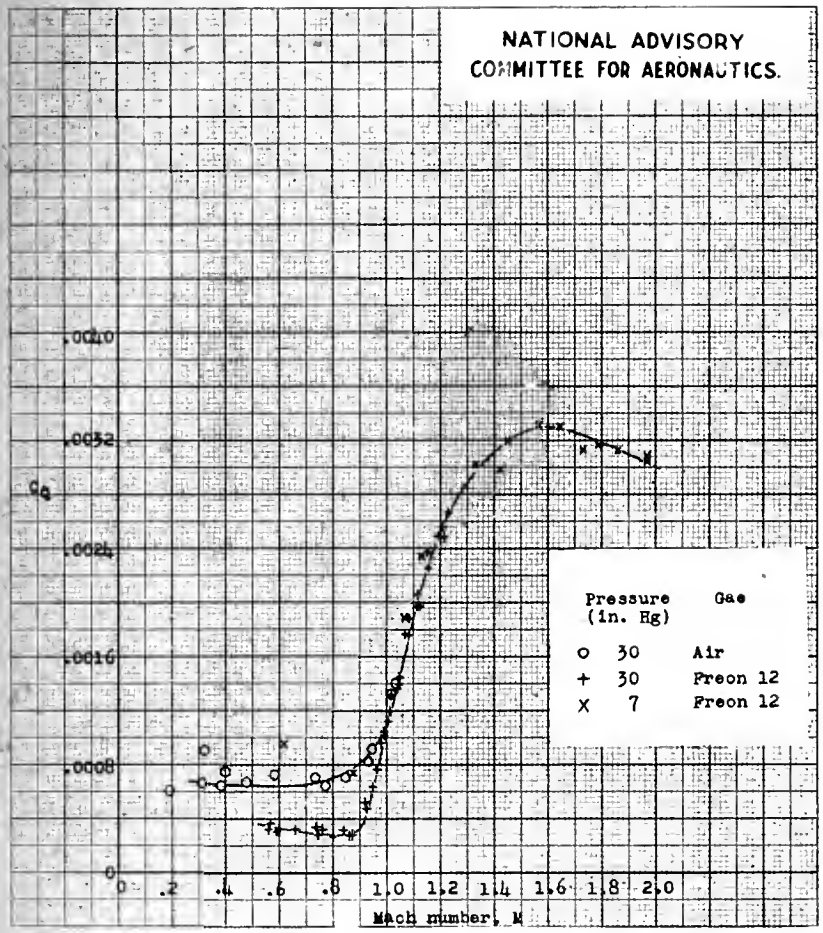

Figure 12.- Torque coefficient $C_Q = \frac{Q}{\rho n^2 D^5}$ as function of Mach number for propeller E.

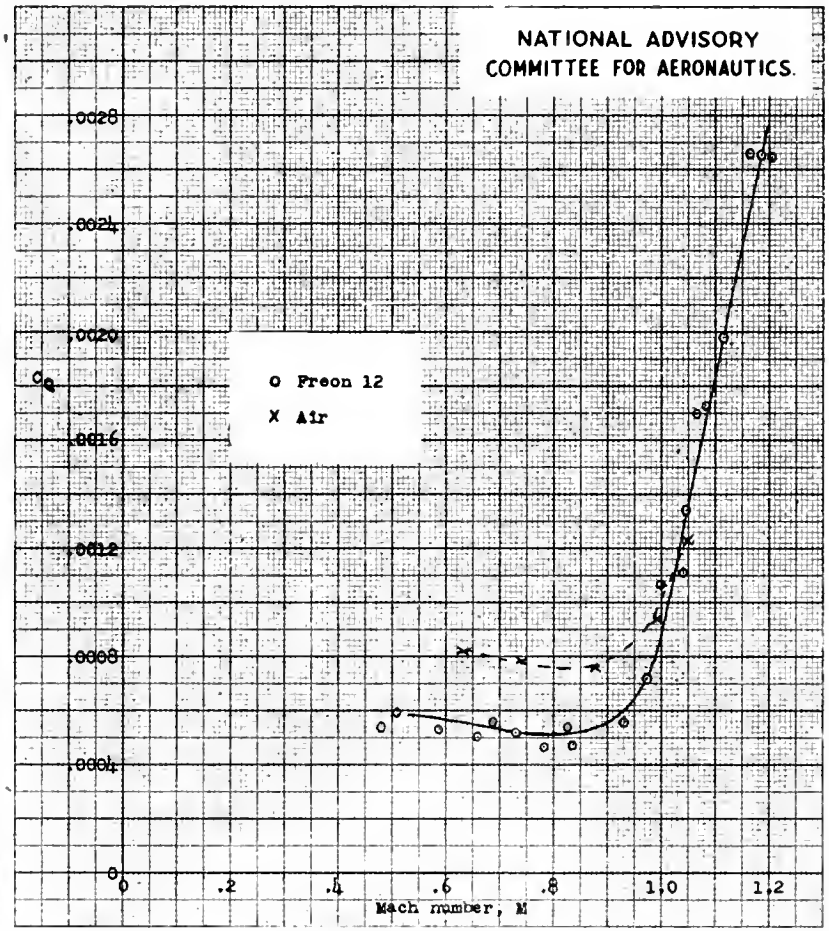

Figure 13.- Torque coefficient $C_Q = \frac{Q}{\rho n^2 D^5}$ as function of Mach number for propeller D.

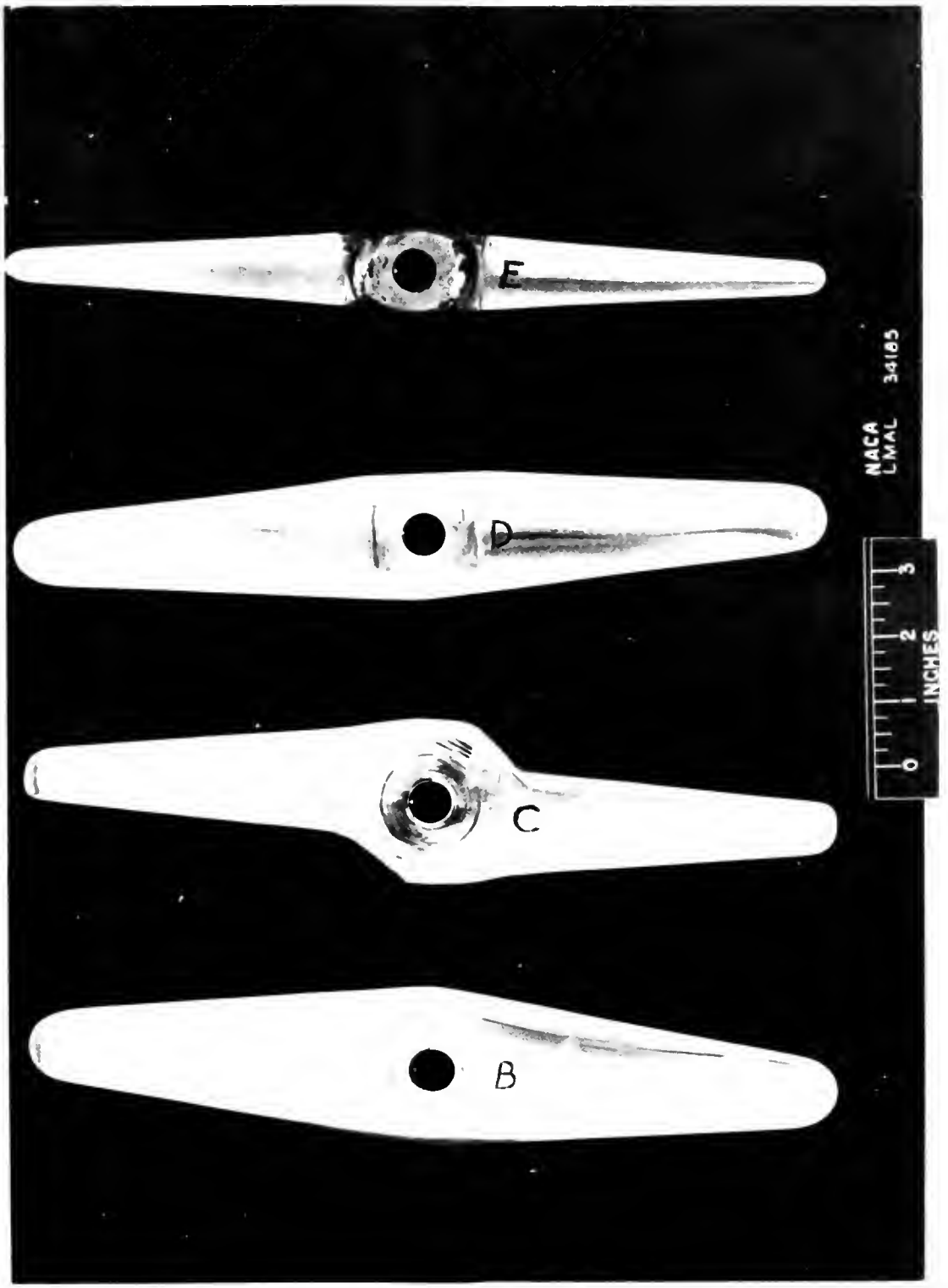

Figure 14. -Propellers B, C, D, and E.

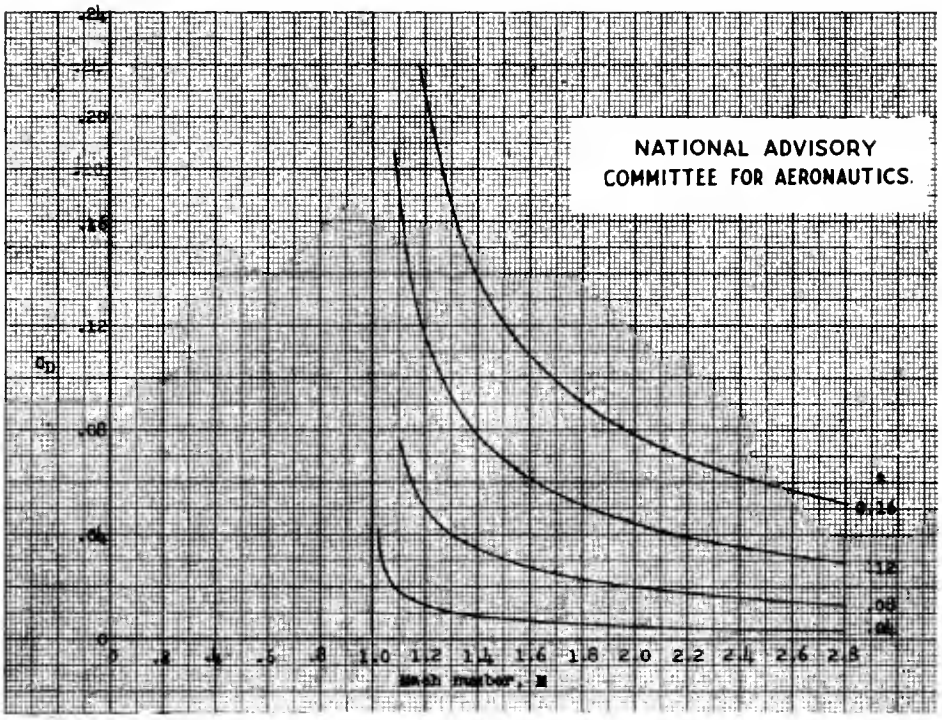

Figure 15.- Theoretical curves of the drag coefficient C_D against Mach number for various thickness ratios for circular-arc airfoils by Ackeret's formula.

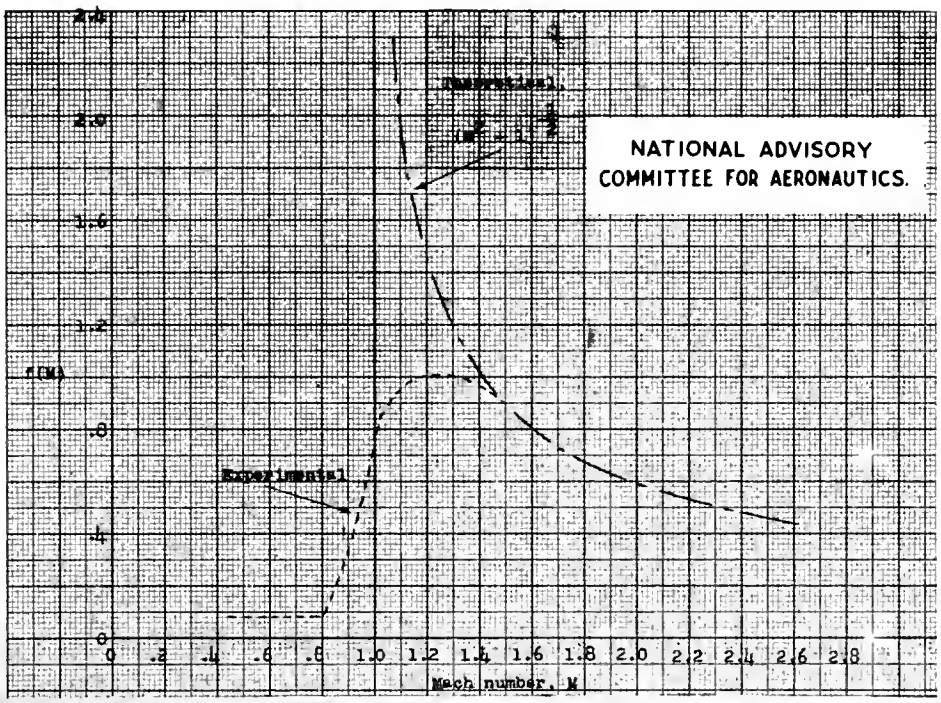

Figure 16.- Values of drag function f(M) as function of Mach number from analysis of experimental moment curves for propeller B in figure 11.

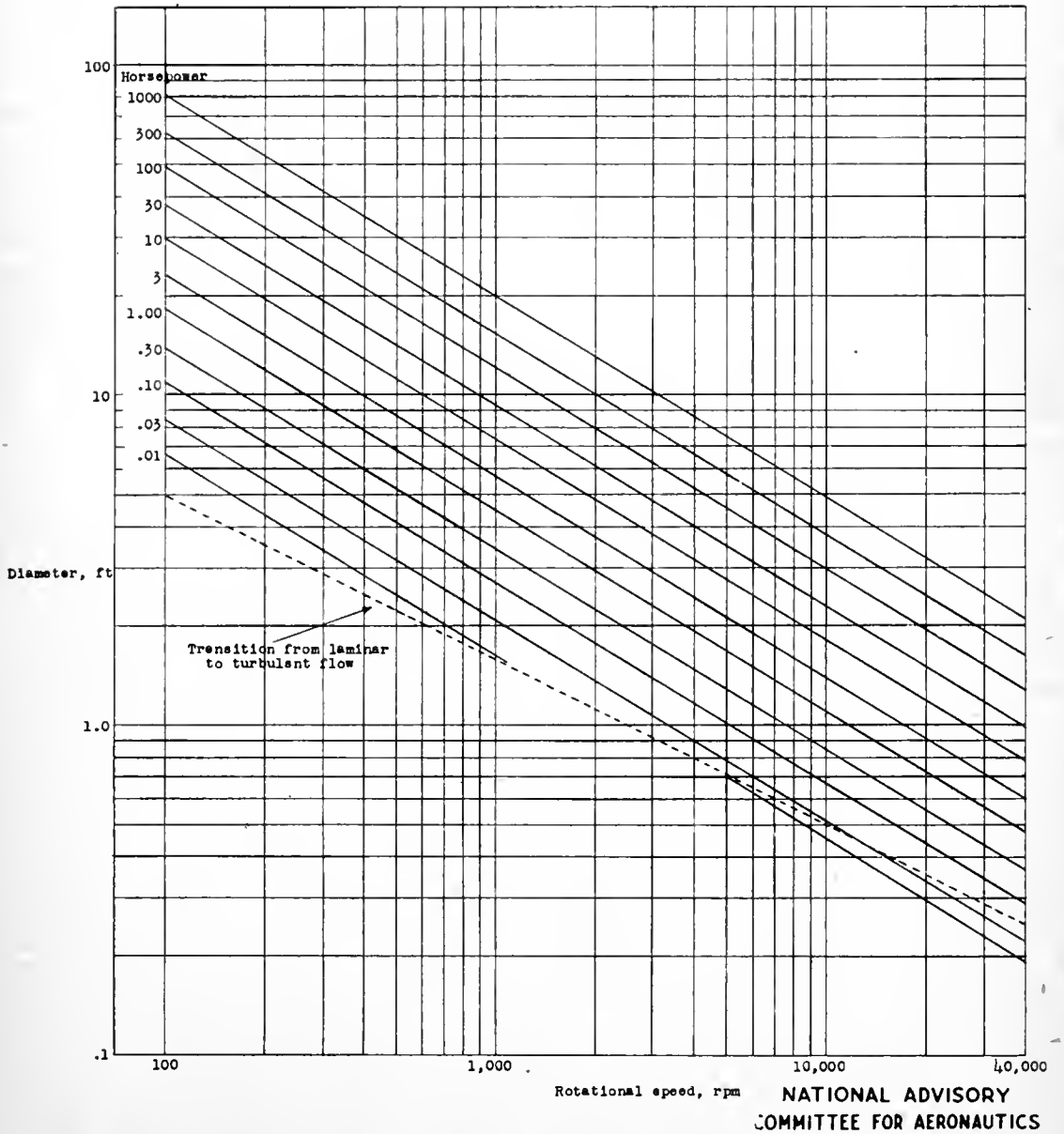

Figure 17.- Power requirement for smooth disks.

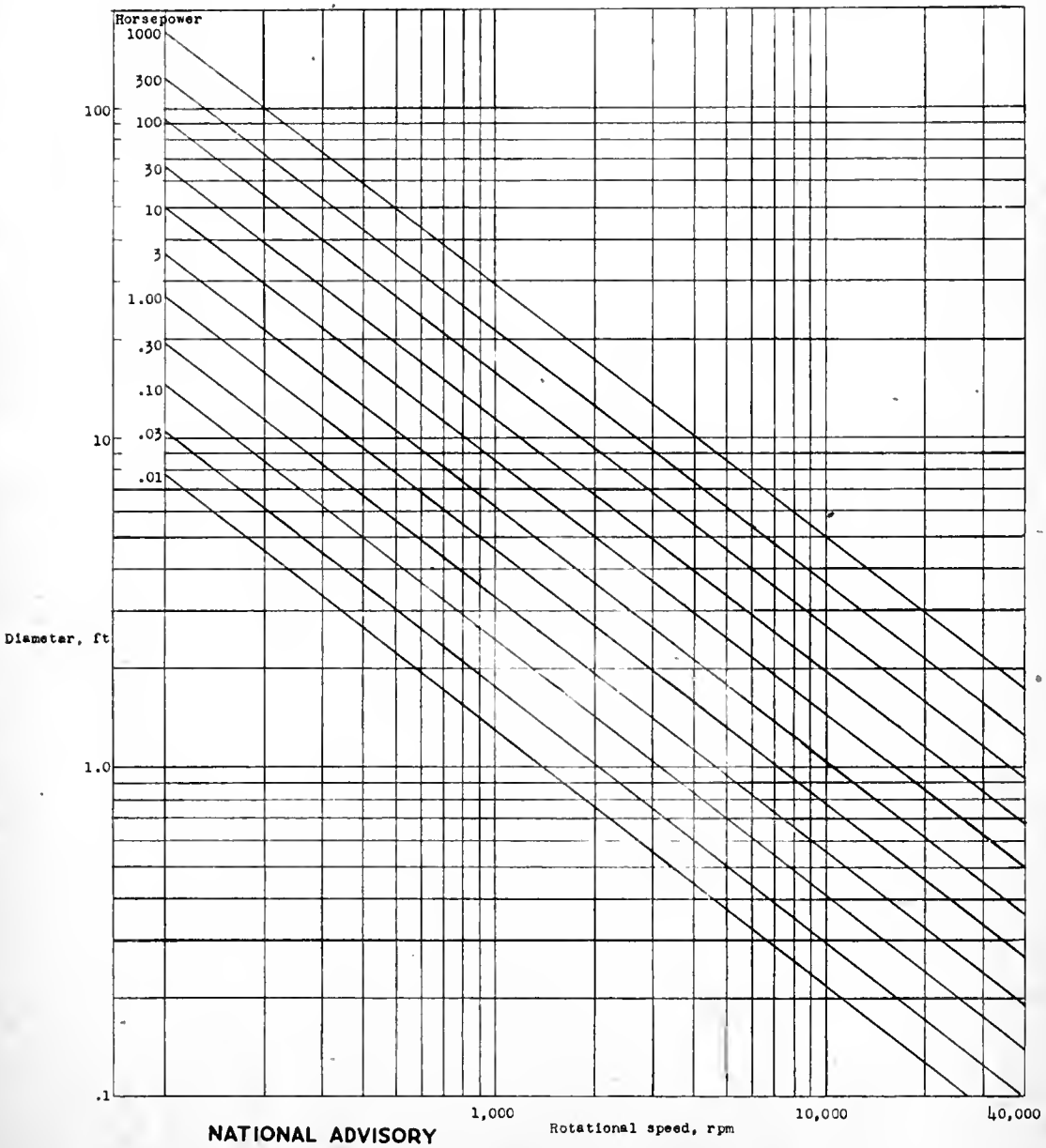

Figure 18.- Power requirement for smooth cylinders (1-ft length).